Eur. Phys. J. A **27**, 105–127 (2006)
DOI 10.1140/epja/i2005-10189-8

THE EUROPEAN PHYSICAL JOURNAL A

Bulk effects in the coherent inelastic scattering of ultracold neutrons

A.L. Barabanov[a] and S.T. Belyaev

Kurchatov Institute, 123182 Moscow, Russia

Received: 1 October 2005 / Revised version: 7 December 2006 /
Published online: 30 January 2006 –
Communicated by R. Krücken

Abstract. With the use of a theory developed earlier, bulk effects in ultracold neutron coherent inelastic scattering are considered both for solid and liquid target samples related to energy and momentum exchange with phonon and diffusion-like modes. For the neutron in a material trap, differential and integral probabilities for the energy transfer per bounce are presented in a simple analytic form which exhibits parameter dependence. As an example, the theoretical values for the ultracold-neutron loss rate from a storage bottle with Fomblin-coated walls and stainless-steel walls are evaluated. A possible contribution from incoherent inelastic scattering is discussed.

PACS. 28.20.-v Neutron physics – 61.12.-q Neutron diffraction and scattering – 89.90.+n Other topics in areas of applied and interdisciplinary physics

1 Introduction

In the last few decades since the discovery [1,2] of ultracold neutrons (UCN), great progress has been made in this field of physics. Now one considers UCN not only as a tool for studying fundamental properties of neutrons (lifetime and electric dipole moment) but also as a method for investigating material surfaces and thin films [3,4].

The main specific feature of UCN is their repulsion from material samples, which allows their storage for a long time in material vessels. This repulsion results from the rescattering of the neutron wave in matter. Indeed, each atom in the target sample feels not only the incoming neutron wave but also the secondary waves from the other atoms. Effective secondary waves come mainly from the surrounding volume $\sim \lambda^3$, where all $\sim n\lambda^3$ scatterers add coherently onto an amplitude $\sim n\lambda^3(b/\lambda)$ (λ is the neutron wavelength, b is the neutron-nucleus scattering amplitude, and n is the density of scatterers). This amplitude may be neglected, as compared to the incoming neutron wave, if $nb\lambda^2 \ll 1$. This is just the case for thermal and cold neutrons but it is not true for ultracold neutrons. Thus, for ultracold neutrons rescattering in matter is of crucial importance, and for the wave vector $k < \sqrt{4\pi nb}$ (if $b > 0$) rescattering becomes the dominant process and results in the total reflection from the surface. This dominant elastic scattering is simply described by a mirror potential $U = 2\pi\hbar^2 nb/m$, where m is the neutron mass.

[a] e-mail: barab@mbslab.kiae.ru

Inelastic scattering of UCN on the trap walls also takes place and, in particular (along with β-decay and radiative capture) results in UCN losses from the material vessels. For a long time attention was focused on the inelastic transition of UCN to the thermal energy region (upscattering), *i.e.* on large energy transfers (with probabilities per bounce 10^{-6} and higher). In the last few years inelastic scattering with small energy transfers ("small heating" and "small cooling") was observed with probabilities per bounce 10^{-8}–10^{-5} (see, *e.g.*, [5–9]).

Therefore, inelastic UCN scattering is now of great interest, first due to the storage of UCN in material traps and, second, for possible spectroscopic applications, *e.g.* for investigation of low-frequency modes in surface layers and thin films [4]. On the other hand, theoretical tools for the calculation of the inelastic scattering of UCN are rather undeveloped. One usually starts from Van Hove formula [10] for the differential cross-section of neutron inelastic scattering on an ensemble of target nuclei,

$$\frac{\mathrm{d}^2\sigma}{\mathrm{d}\omega\mathrm{d}\Omega} = \frac{k'}{2\pi k}\sum_{\nu,\nu'} b_\nu^* b_{\nu'} \int\limits_{-\infty}^{+\infty} \mathrm{d}t\, e^{i\omega t}\langle i|e^{-i\mathbf{Q}\hat{\mathbf{R}}_\nu(t)} e^{i\mathbf{Q}\hat{\mathbf{R}}_{\nu'}(0)}|i\rangle. \tag{1}$$

Here and below we assume that $\mathbf{k}$ ($\varepsilon = \hbar^2 k^2/2m$) and $\mathbf{k}'$ ($\varepsilon' = \hbar^2 k'^2/2m$) are the wave vectors (energies) for incident and scattered neutrons, respectively, $\hbar\omega = \varepsilon - \varepsilon'$ and $\mathbf{Q} = \mathbf{k} - \mathbf{k}'$ are the neutron energy and momentum transfers, $\hat{\mathbf{R}}_\nu(t)$ is the time-dependent Heisenberg operator of the ν-th nucleus position vector, and b_ν is the scattering

amplitude on the ν-th nucleus. The averaging is understood over the initial state $|i\rangle$ of the nuclear ensemble.

Note, however, that the Van Hove formula (1) is based on the Born approximation (see, *e.g.*, [11,12]) and, hence, does not imply rescattering. Strictly speaking, it may be applied only to thermal and cold neutrons (see also [13]).

Nevertheless, it is being used for UCN as the starting point for some tricky ansatz. First, one notes that the inelastic cross-section, both for coherent and incoherent scattering, predicted by (1) is proportional to the total number of nuclei in the target. This allows to introduce the inelastic cross-section for one nucleus. It should be stressed that this definition is purely formal, because in fact the neutron is scattered by the whole sample as directly indicated by the presence of the correlation function in the right-hand side of (1). Then, the resulting cross-section for neutron-nucleus scattering may be somehow extrapolated from the cold to the ultracold energy region (say assuming $1/v$ law). The sum of this inelastic cross-section and that for the radiative capture on one nucleus is considered as the cross-section of the total loss, which is supposed to define the imaginary part of the matter optical potential (see, *e.g.*, [14,15]). Some model modification of the Van Hove theory for UCN was attempted in [16].

Note that the observed UCN losses are, as a rule, higher than that theoretically expected. With this respect one uses the term "UCN anomalous losses" (see, *e.g.*, [17, 18][1]). In fact, while one speaks of a discrepancy between experiment and theory, there is really a lack of a reliable theoretical description for UCN losses. We would like to emphasize that the rescattering results in a drastic change in elastic neutron scattering when one goes from the cold to the ultracold region. Thus, one can expect an important influence of this transition on inelastic scattering. Thus, a theory of the inelastic scattering of UCN, based on solid grounds is, certainly, needed.

Recently, the present authors presented a general theory of neutron scattering [13], valid for the whole domain of slow neutrons from thermal to ultracold. In this theory the amplitude of the neutron wave, ϕ, due to rescattering, is different at each nucleus, ν, of the sample and depends on the energy already transferred, *i.e.* on the target sample state, j. In other words, the quantity ϕ_ν^j is the neutron amplitude on the surface of the ν-th nucleus provided that the target sample is at the state j. These amplitudes are determined by a set of linear equations. The differential cross-section takes the form

$$\frac{\mathrm{d}^2\sigma}{\mathrm{d}\omega \mathrm{d}\Omega} = \frac{k'}{2\pi k} \sum_{\nu,\nu'} \sum_{j,j'} \phi_\nu^{j*} \phi_{\nu'}^{j'} \times \int_{-\infty}^{+\infty} \mathrm{d}t\, e^{i\omega t + i(\varepsilon_i - \varepsilon_j)t/\hbar} \langle j| e^{-i\mathbf{Q}\hat{\mathbf{R}}_\nu(t)} e^{i\mathbf{Q}\hat{\mathbf{R}}_{\nu'}(0)} |j'\rangle. \quad (2)$$

It was shown that for thermal and cold neutrons, when rescattering is not important, the equations for ϕ_ν^j become very simple and result in $\phi_\nu^j \simeq \delta_{ij} b_\nu$. Thus, the cross-section takes the Van Hove form (1). For the opposite case of ultracold neutrons, when rescattering becomes the dominant process, we have solved the equations for the amplitudes ϕ_ν^j. These amplitudes were presented as expansions in a small parameter $\mathbf{Qu}$, where $\mathbf{u}_\nu$ is the shift from the equilibrium position $\boldsymbol{\rho}_\nu$ of the ν-th nucleus in the target sample ($\mathbf{R}_\nu = \boldsymbol{\rho}_\nu + \mathbf{u}_\nu$).

The zeroth order in $\mathbf{Qu}$ corresponds to the scattering on the target sample with fixed, frozen (or infinitely heavy) nuclei and evidently it can describe only elastic scattering. For inelastic scattering, one should consider the next orders in the small parameter $\mathbf{Qu}$. It is convenient to introduce the renormalized neutron amplitudes $\psi_j(\nu) \equiv e^{i\mathbf{k}\boldsymbol{\rho}_\nu} \phi_\nu^j / \beta_\nu$, and present them as series in $\mathbf{Qu}$:

$$\psi_j(\nu) = \delta_{ij}\psi(\nu) + \psi_j^{(1)}(\nu) + \dots \quad (3)$$

Here β_ν is the scattering length on the bound nucleus [13] (this quantity slightly differs from b_ν).

Zeroth-order amplitudes $\psi(\nu) = \psi(\boldsymbol{\rho}_\nu)$ in the continuous-medium approximation were found to satisfy the Schroedinger equation with the optical potential $U(\boldsymbol{\rho}) = 2\pi\hbar^2 n(\boldsymbol{\rho})\beta_c/m$, where β_c is the average ("coherent") scattering amplitude. Thus, the solution $\psi(\mathbf{k}, \boldsymbol{\rho}_\nu)$ determines the zeroth-order neutron amplitude on the surface of the ν-th nucleus inside a sample provided that the incident neutron has the wave vector $\mathbf{k}$.

Dynamical properties of the sample, and therefore inelastic scattering, arise in the first order in $\mathbf{Qu}$. The corresponding cross-section on the whole target (even on a macroscopic one) was obtained in the form

$$\frac{\mathrm{d}^2\sigma_{ie}}{\mathrm{d}\omega \mathrm{d}\Omega} \sim \sum_{\nu,\nu'} \beta_\nu^* \beta_{\nu'} \nabla_\nu^i \left(\bar{\psi}(\mathbf{k}', \nu)\psi(\mathbf{k}, \nu)\right)^* \times \nabla_{\nu'}^j \left(\bar{\psi}(\mathbf{k}', \nu')\psi(\mathbf{k}, \nu')\right) \int_{-\infty}^{+\infty} \langle i|\hat{u}_\nu^i(t)\hat{u}_{\nu'}^j(0)|i\rangle e^{i\omega t} \mathrm{d}t, \quad (4)$$

where $\bar{\psi}(\mathbf{k}, \nu) = \psi(-\mathbf{k}, \nu)$ is to be interpreted as the wave function in the exit channel. Needless to say that the cross-section (4) should be averaged over target initial states $|i\rangle$ with thermal equilibrium density matrix. Below, such averaging is implied.

The purpose of this paper is to demonstrate a real possibility to use our approach for the analysis of the results of experiments on UCN inelastic scattering during their storage into material vessels. Corresponding observables for both large and small energy transfers are discussed in sect. 2. Since the energies of initial neutrons are less than the barrier energy U, the function $\psi(\mathbf{k}, \boldsymbol{\rho})$ decreases rapidly inward from the surface of the target, namely at a length on the scale of 10 nm. Then, clearly, the notions like the total number of nuclei scatterers and the inelastic cross-section for one nucleus are senseless. We are not introducing them. In this sense, our approach is quite different from that commonly used for UCN [14,15].

As a first step we assume that at an intrusion length $\sim$ 10 nm the bulk properties of the matter are of domi-

[1] See also comments [19,20] on the article [18].

nant importance (for a discussion of the surface effects in the inelastic scattering, *e.g.*, the contribution from viscoelastic waves for Fomblin oil or from hydrogen thin films, see [4,21–23]). Thus, in a uniform material the diagonal matrix element $\langle i|\hat{u}^i_\nu(t)\hat{u}^j_{\nu'}(0)|i\rangle$ may exhibit a spatial dependence only as a function of $\boldsymbol{\rho}_\nu - \boldsymbol{\rho}_{\nu'}$ and therefore allows a Fourier transform

$$\langle i|\hat{u}^i_\nu(t)\hat{u}^j_{\nu'}(0)|i\rangle = \sum_{\mathbf{q},\omega} e^{i\mathbf{q}(\boldsymbol{\rho}_\nu-\boldsymbol{\rho}_{\nu'})-i\omega t}\Omega^{ij}(\mathbf{q},\omega), \qquad (5)$$

where $\sum_{\mathbf{q}} = \int \mathrm{d}^3q/(2\pi)^3$ and $\sum_\omega = \int \mathrm{d}\omega/2\pi$. The correlation function $\Omega^{ij}(\mathbf{q},\omega)$ for the target material is the most uncertain factor in our approach. We analyze it in sect. 3.

In expression (4) we take into account all terms with $\nu \neq \nu'$ (as well as with $\nu = \nu'$), *i.e.* we calculate the coherent contribution to inelastic scattering. Thus, we use the average value (coherent scattering length) β_c instead of β_ν in expressions for the inelastic cross-section derived from (4). Note that to evaluate the incoherent contribution related both to spin-flip and mixture of nuclei with different scattering lengths, one needs to separate the additional term (proportional to β^2_{inc}) from the general equation (4) keeping only $\nu = \nu'$.

In this paper we restrict ourselves to coherent inelastic scattering. Thus, we realize that our consideration is unsuitable for the treatment of neutron scattering on targets with high hydrogen contamination. Our goal is the application to "hydrogen-free" materials, *e.g.* to Fomblin oil. On the other hand, even for such materials we do not aspire to a quantitative description of the experimental data. They may be defined predominantly by surface effects and non-hydrogen incoherent-scattering contributions.

Our main purpose is to study the relative contributions of "fast" (phonon or sound) and "slow" (diffusion-like) modes to large and small energy transfer processes both for solids and liquids. It is well known that for crystals, the dominating contribution to the upscattering (into the thermal region) is due to phonon processes with momentum transfer to the lattice (see, *e.g.*, [17]). On the other hand, non-lattice processes (both "fast" and "slow") are responsible for small energy transfers in crystals and any energy transfers in liquids and amorphous matter. They are all considered in detail in this paper.

As the starting point we use the following expression for the coherent inelastic cross-section on the whole target [13]:

$$\frac{\mathrm{d}\sigma_{ie}}{\mathrm{d}^3k'} = \frac{\hbar}{2\pi mk}\sum_{\mathbf{q}} B^{i*}(\mathbf{q})B^j(\mathbf{q})\Omega^{ij}(\mathbf{q},\omega), \qquad (6)$$

where

$$\mathbf{B}(\mathbf{q}) = \beta_c \sum_\nu e^{-i\mathbf{q}\boldsymbol{\rho}_\nu}\boldsymbol{\nabla}_\nu\left(\bar{\psi}(\mathbf{k}',\nu)\psi(\mathbf{k},\nu)\right). \qquad (7)$$

It describes the transition of an incident neutron with the wave vector $\mathbf{k}$ into an element d^3k' of the final wave vector space $\mathbf{k}'$. This equation is valid for neutrons in a broad energy region, since the smallness of the parameter $\mathbf{Qu}$, that was used for deriving eq. (6), is valid even for thermal neutrons. Indeed, for the latter, the scattering on the optical potential ($\sim$ 100 neV) is not important. Then, if one replaces the functions $\psi(\mathbf{k},\boldsymbol{\rho})$ and $\bar{\psi}(\mathbf{k}',\boldsymbol{\rho})$ by the plane waves $e^{i\mathbf{k}\boldsymbol{\rho}}$ and $e^{-i\bar{\mathbf{k}}'\boldsymbol{\rho}}$, respectively, then (6) takes the form (1).

In this paper we consider the inelastic scattering of initial ultracold neutrons to any final energies, below and above the potential barrier. Of course, to calculate the neutron inelastic cross-section from (6) and (7) one needs a specific model for the target sample to find the solutions $\psi(\mathbf{k},\boldsymbol{\rho})$ and $\bar{\psi}(\mathbf{k}',\boldsymbol{\rho})$ for input and output channels. This problem is considered in sect. 4.

In sect. 5 it is shown that multi-dimensional integration in (6) and (7) can be performed explicitly with realistic correlation functions. The details of the calculation are presented in the appendix. In sect. 6 we analyze how analytical results for the differential probability are changed when specified for the excitation mode and energy transfer. In sect. 7 numerical results are presented for two typical substances, stainless steel and Fomblin oil. The results obtained, both analytical and numerical, are discussed in sect. 8. Conclusion is given in sect. 9.

2 Inelastic scattering of UCN in material trap

The probability for energy transfer per bounce is naturally defined as the ratio of two cross-sections, the differential for energy transfer and the integral elastic one. The latter, in our case, is equal simply to the total sample area seen by the neutron, $S_\perp = Sk_\perp/k = S\cos\theta$, θ is the angle of incidence. With fixed initial wave vector $\mathbf{k}$ (or its two components $k_\perp$ and $k_\parallel$), the probability for the neutron after a bounce to have the kinetic energy ε' is

$$\frac{\mathrm{d}w(k_\perp,k_\parallel\to\varepsilon')}{\mathrm{d}\varepsilon'} = \frac{1}{S_\perp}\int \frac{\mathrm{d}\sigma_{ie}}{\mathrm{d}^3k'}\,\frac{\mathrm{d}^3k'}{\mathrm{d}\varepsilon'}. \qquad (8)$$

However, in the storage experiments one usually measures quantities somehow averaged over the initial momentum $\mathbf{k}$. Let us introduce a quasi-classical distribution $F(\mathbf{r},\mathbf{k})$ in position $\mathbf{r}$ and momentum $\mathbf{k}$ of UCN inside the trap, normalized by the condition

$$\int \mathrm{d}^3r \int \mathrm{d}^3k\, F(\mathbf{r},\mathbf{k}) = N_0, \qquad (9)$$

where N_0 is the total number of UCN in the trap.

The number of neutrons, scattered by the element $\mathrm{d}\mathbf{S}$ of the material sample at the position $\mathbf{r}_S$ (and height h_S) to the interval $\mathrm{d}E'$ of the total energy $E' = \varepsilon' + mgh_S$ during the time $\mathrm{d}t$, is given by

$$\mathrm{d}N = \mathrm{d}E'\mathrm{d}t \int \mathrm{d}^3k\, F(\mathbf{r}_S,\mathbf{k})\ (\mathbf{v}\mathrm{d}\mathbf{S}) \times \frac{\mathrm{d}w(k_\perp,k_\parallel\to E'-mgh_S)}{\mathrm{d}E'}, \qquad (10)$$

where $\mathbf{v} = \hbar\mathbf{k}/m$ is the neutron velocity, and mgh_S is the neutron potential energy in the Earth's gravitational field. The total rate of inelastic transition to the energy interval $\mathrm{d}E'$ is of the form

$$\frac{\mathrm{d}N(E')}{\mathrm{d}E'\mathrm{d}t} = \oint \mathrm{d}S \int\limits_{k_\perp>0} \mathrm{d}^3k\, v_\perp F(\mathbf{r}_S, \mathbf{k}) \times \frac{\mathrm{d}w(k_\perp, k_\parallel \to E' - mgh_S)}{\mathrm{d}E'}. \quad (11)$$

Let us assume that the momentum distribution is isotropic, *i.e.* $F(\mathbf{r}, \mathbf{k}) = F(\mathbf{r}, k)$. Then, it is convenient to introduce a distribution $f(\mathbf{r}, \varepsilon)$ in position and kinetic energy of UCN inside the trap

$$f(\mathbf{r}, \varepsilon) = 2\pi \left(\frac{2m}{\hbar^2}\right)^{3/2} \sqrt{\varepsilon}\, F(\mathbf{r}, k), \quad k = \sqrt{\frac{2m\varepsilon}{\hbar^2}}, \quad (12)$$

normalized by the condition

$$\int \mathrm{d}^3r \int\limits_0^\infty \mathrm{d}\varepsilon f(\mathbf{r}, \varepsilon) = N_0. \quad (13)$$

Then, the transition rate takes the form

$$\frac{\mathrm{d}N(E')}{\mathrm{d}E'\mathrm{d}t} = \oint \mathrm{d}S \int\limits_0^\infty \mathrm{d}\varepsilon\, v f(\mathbf{r}_S, \varepsilon) \frac{\mathrm{d}w(\varepsilon \to E' - mgh_S)}{\mathrm{d}E'}, \quad (14)$$

where

$$\frac{\mathrm{d}w(\varepsilon \to \varepsilon')}{\mathrm{d}\varepsilon'} = \left\langle \frac{\mathrm{d}w(k_\perp, k_\parallel \to \varepsilon')}{\mathrm{d}\varepsilon'} \right\rangle \quad (15)$$

is the inelastic scattering differential probability averaged over the angle of incidence θ.

Here and below averaging of any function $f(k_\perp, k_\parallel)$ over θ is defined as

$$\langle f(k_\perp, k_\parallel) \rangle = \frac{1}{2} \int\limits_0^{\pi/2} \mathrm{d}\theta \sin\theta \cos\theta\, f(k\cos\theta, k\sin\theta). \quad (16)$$

In the simplest approximation we neglect the Earth's gravitational field, and assume that, first, the density n_U of UCN in the trap is uniform over the volume and, second, the energy of UCN is fixed and equal to ε_U, thus

$$f(\mathbf{r}, \varepsilon) = n_U \delta(\varepsilon - \varepsilon_U). \quad (17)$$

The inelastic transition rate is of the form

$$\frac{\mathrm{d}N(\varepsilon')}{\mathrm{d}\varepsilon'\mathrm{d}t} = S n_U v_U \frac{\mathrm{d}w(\varepsilon_U \to \varepsilon')}{\mathrm{d}\varepsilon'}, \quad (18)$$

where S is the total area of the material surface inside the trap.

When the final neutron energy E' exceeds the barrier energy U, the neutron escapes from the trap. The probability of this event and the corresponding transition rate can be obtained as an integral over E' from U up to infinity from (14) (in the simplest approximation —as the similar integral over ε' from (18)).

3 Correlation function

In this section we consider the correlation function $\Omega^{ij}(\mathbf{q}, \omega)$, entering in eq. (6). Correlation functions describe the response (relaxation) of a substance after distortion of its statistical equilibrium by some external force characterized by ω and $\mathbf{q}$. Their structures for solids and liquids are covered in many books and articles on fluctuations and kinetics (see, *e.g.*, [24–27]). We restrict ourselves to the details necessary for what follows.

Fast distortions (when $|\omega| \gg \tau^{-1}$, where τ is some average relaxation time) are relaxed by phonons (or sound waves). In this region the correlation function can be easily obtained by expansion of the displacement vectors $\hat{\mathbf{u}}^i_\nu(t)$ in phonon amplitudes. The result is well known (see, *e.g.*, eq. (4.26) of ref. [25]):

$$\Omega^{ij}(\mathbf{q}, \omega) = \Omega^{ij}_l(\mathbf{q}, \omega) + \Omega^{ij}_t(\mathbf{q}, \omega), \quad (19)$$

where the longitudinal and transverse parts are given by

$$\Omega^{ij}_l(\mathbf{q}, \omega) = \frac{q_i q_j}{q^2} \Omega_l(q, \omega), \quad (20)$$

$$\Omega^{ij}_t(\mathbf{q}, \omega) = \left(\delta_{ij} - \frac{q_i q_j}{q^2}\right) \Omega_t(q, \omega), \quad (21)$$

and

$$\Omega_{l,t}(q, \omega) = \frac{2\hbar n_0(\omega)}{\rho c^2_{l,t}} \frac{\Gamma^2_{l,t}}{(q^2 - \omega^2/c^2_{l,t})^2 + \Gamma^4_{l,t}}. \quad (22)$$

Here $\rho = Mn$ is the material density (M is the nuclear mass), and

$$n_0(\omega) = \frac{1}{\exp(\hbar|\omega|/T) - 1} \underset{\hbar|\omega| \ll T}{\simeq} \frac{T}{\hbar|\omega|} \quad (23)$$

is the occupation factor for a mode with the frequency ω at the temperature T. We allow the longitudinal (l) and transverse (t) sound velocities $c_{l,t}$ and damping factors $\Gamma_{l,t}$ to be different.

For isotropic solids, the factors $\Gamma^2_{l,t}$ can be taken proportional to the absorption coefficients of longitudinal and transverse sound (see, *e.g.*, [28])

$$\Gamma^2_l = \frac{\gamma|\omega|^3}{c^4_l}, \qquad \gamma = \frac{\zeta}{\rho} + \alpha D_S, \quad (24)$$

$$\Gamma^2_t = \frac{\nu|\omega|^3}{c^4_t}, \qquad \nu = \frac{\eta}{\rho}. \quad (25)$$

Here η and $\zeta = 4\eta/3 + \varphi$ are the dynamic shear and longitudinal viscosities (φ is the volume viscosity), ν is the kinematic viscosity, $\alpha = C_P/C_V - 1$, where C_P and C_V are the specific heats for constant pressure and volume, respectively, $D_S = æ/\rho C_P$ is the thermo-diffusion coefficient (æ is the thermo-conductivity).

To describe a small energy exchange between UCN and a sample, the form of the correlation function for small ω and q is of prime interest. Slow- and long-range fluctuations are related to the coherent motion of a

great number of atoms (hydrodynamic modes). For such kinds of distortion, local statistical equilibrium comes first and macro-relaxation by hydrodynamic processes follows. Therefore, in the region of small ω and q correlation functions for solids and liquids are governed by hydrodynamics and should depend on its parameters. Two different approaches, namely, phenomenological (from hydrodynamic fluctuations and Kubo theory [24,25]) and quantum many-body theory [29], give the same result. In hydrodynamics two kinds of processes (and corresponding correlations) are distinguished, longitudinal and transverse.

The longitudinal correlation function is related to "density-density" fluctuations

$$\frac{1}{2\pi N}\left\langle \int \hat{n}(\mathbf{r}'+\mathbf{r},t)\,\hat{n}(\mathbf{r}',0)\mathrm{d}\mathbf{r}' \right\rangle = \sum_{\mathbf{q},\omega} e^{i\mathbf{q}\mathbf{r}-i\omega t} S(\mathbf{q},\omega), \tag{26}$$

where a Fourier transform, the "dynamical structure factor", can be shown to be connected with $\Omega_l(\mathbf{q},\omega)$ by

$$S(\mathbf{q},\omega) \simeq \frac{nq^2}{2\pi}\Omega_l(\mathbf{q}',\omega). \tag{27}$$

The vector $\mathbf{q}'$ in Ω_l is in the first Brillouin zone and $\mathbf{q}$, the momentum transfer, may differ from $\mathbf{q}'$ by a reciprocal lattice vector. In the right-hand side of (27), we omit all terms proportional to $\delta(\omega)$ and related to elastic scattering.

Following [24,25] we get for both solids and liquids

$$\Omega_l(q,\omega) = \frac{T}{i\rho\omega}\left(\frac{1}{\omega^2 - c_{lT}^2 q^2 - i\omega\Gamma_l(q,\omega)} - \text{c.c.}\right), \tag{28}$$

which looks like a phonon type but with the complicated form of "phonon absorption"

$$\Gamma_l(q,\omega) = \frac{(c_{lS}^2 - c_{lT}^2)q^2}{D_T q^2 + i\omega} + \frac{\zeta q^2}{\rho}, \tag{29}$$

where D_T is the thermo-diffusion coefficient. The subscripts T and S indicate constant temperature and entropy, respectively, and

$$\frac{c_{lS}^2}{c_{lT}^2} = \frac{D_T}{D_S} = \frac{C_P}{C_V} = 1+\alpha. \tag{30}$$

For $q^2 \ll |\omega|/D_T$, eqs. (28) and (29) result in the pure phonon-type correlation function with the sound velocity c_{lS} and the absorption defined by (24). For arbitrary small ω and q (hydrodynamic region)

$$|\omega| \ll \frac{c_l^2}{\gamma}, \qquad q \ll \frac{c_l}{\gamma}, \tag{31}$$

the function (28) takes the form

$$\Omega_l(q,\omega) = \frac{iT}{\rho\omega} \times \left(\frac{q^2 + i\omega/D_T}{c_{lT}^2(q^2+i\omega/D_S)(q^2-\omega^2/c_{lS}^2 + i\omega^3\gamma/c_{lS}^4)} - \text{c.c.}\right). \tag{32}$$

It has two kinds of poles, of phonon (p) and of thermo-diffusion (d) origin, and it is useful to separate them as

$$\Omega_l(q,\omega) = \Omega_l^p(q,\omega) + \Omega_l^d(q,\omega). \tag{33}$$

Here $\Omega_l^p(q,\omega)$ is given by (22) with Γ_l^2 (24) and

$$\Omega_l^d(q,\omega) = \frac{2T}{\rho c_{lS}^2|\omega|}\,\frac{\alpha\Gamma_d^2}{q^4+\Gamma_d^4}, \qquad \Gamma_d^2 = \frac{|\omega|}{D_S}. \tag{34}$$

It is easy to see that the additional diffusion-type pole in (32) originates from the pole in the "phonon absorption" $\Gamma_l(q,\omega)$ (29). The complicated structure of $\Gamma_l(q,\omega)$ is intrinsic only for longitudinal phonons.

The transverse correlation function for solids has only one, phonon-like, pole. So, transverse excitations in solids are relaxed only by phonons, and the correlation function for small ω and q has the same form (22) as for large q and ω.

In common liquid models, kinetics is assumed to go by finite jumps of atoms from one equilibrium position to the other after some average waiting time τ. For high frequencies $|\omega| \gg \tau^{-1}$ a liquid behaves like a solid. Low-frequency waves ($|\omega| \ll \tau^{-1}$) damp due to viscosity. This limit is reproduced by the correlation function for the liquid model with one relaxation time (see, *e.g.*, [24])

$$\Omega_t(q,\omega) = \frac{T}{i\rho c_t^2 q^2}\left(\frac{1}{\omega - i\Gamma_t(q,\omega)} - \text{c.c.}\right), \tag{35}$$

where

$$\Gamma_t(q,\omega) = \frac{c_t^2 q^2 \tau}{1+i\omega\tau}. \tag{36}$$

The relaxation time is usually estimated as $\tau = \eta/G = \nu/c_t^2$, where η and $\nu = \eta/\rho$ are the dynamic and kinematic shear viscosities, respectively, G is the modulus of elasticity, and $c_t^2 = G/\rho$.

The correlation function (35) and (36) exactly takes the form (22) with the damping factor

$$\Gamma_t^2 = \frac{|\omega|}{c_t^2\tau} = \frac{|\omega|}{\nu}. \tag{37}$$

Note that for low frequencies,

$$|\omega| \ll \tau^{-1} = \frac{c_t^2}{\nu}, \tag{38}$$

there exists a wide hydrodynamic region for q,

$$\frac{|\omega|}{c_t} \ll q \ll \frac{c_t}{\nu}, \tag{39}$$

where eq. (35) (as well as (22)) transforms into the diffusion-type function (34) with damping factor (37). It is of interest that this factor is proportional to ν^{-1} in contrast to (25) (see, *e.g.*, [30]).

The correlation functions can be determined from first principles only for two limiting areas of variables, large and small ω and $\mathbf{q}$. In the intermediate area one should

use some specific interpolation models for the substance considered.

Thus, we use the correlation function as a sum of phonon- and diffusion-type terms. The contribution to the cross-section from each part can be calculated independently and summed afterwards.

For the calculation of the cross-section we will need $\Omega(\mathbf{q},\omega)$ as a function of $q_\perp$ ($q^2 = q_\perp^2 + q_\parallel^2$), and it is convenient to present all cases considered above in the same form

$$\Omega(q_\perp) = \frac{2\alpha\hbar n_0(\omega)}{\rho c^2}\bar{\Omega}(q_\perp), \tag{40}$$

where

$$\bar{\Omega}(q_\perp) = \frac{\Gamma^2}{(q_\perp^2+p^2)^2+\Gamma^4}, \qquad p^2 = q_\parallel^2 - \frac{\epsilon\,\omega^2}{c^2}, \tag{41}$$

and $\alpha = \epsilon = 1$ for all cases besides the longitudinal thermo-diffusion mode. In the latter case, we have $\alpha = C_P/C_V - 1$ and $\epsilon = 0$.

Note that Γ_p^2 (phonon absorption) is a small parameter for all values of ω and q that we are considering, and when $\Gamma_p \to 0$,

$$\bar{\Omega}_p(q_\perp) \quad \longrightarrow \quad \pi\delta\left(q^2 - \frac{\omega^2}{c^2}\right), \tag{42}$$

in agreement with the phonon correlation function usually used.

4 Uniform thick layer as a target sample

In this section we will derive the function $\mathbf{B}(\mathbf{q})$ (7) for a simple model commonly relevant to the UCN storage experiments, *i.e.* a uniform thick layer. The appropriate choice of the model allows us to define the solutions $\psi(\mathbf{k},\boldsymbol{\rho})$ and $\bar{\psi}(\mathbf{k}',\boldsymbol{\rho})$ of the Schroedinger equation with optical potential for input and output channels.

The problem is that the function $\psi(\mathbf{k},\nu)$, being the neutron amplitude at the ν-th nucleus, is defined only inside the sample. But to get $\psi(\mathbf{k},\nu)$ in the continuous-medium approximation, one has to find the scattering type solution of the Schroedinger equation with an external plane wave entering the sample, $e^{i\mathbf{k}\boldsymbol{\rho}}$. For the input channel function, $\psi(\mathbf{k},\nu)$, one may imagine the external plane wave as attributed to the incoming neutron. Let us assume it to come from the left. For the output channel function, $\bar{\psi}(\mathbf{k}',\boldsymbol{\rho}) = \psi(-\mathbf{k}',\boldsymbol{\rho})$, the corresponding external wave, $e^{-i\mathbf{k}'\boldsymbol{\rho}}$, is an auxiliary quantity and should be directed to the right, for back scattering, and to the left, for forward scattering.

To include both cases, let us consider a uniform layer located at $-a/2 < z < a/2$ with surface area S and thickness a, much larger than the incident neutron wavelength. The sample is supposed to have density n and scattering length β_c providing a constant optical potential U. Note that in a general case, β_c is complex with an imaginary part that can be used to describe the radiative capture of UCN.

We consider two solutions of the model scattering problem, described above, with the left (L) and right (R) incoming waves. Outside the target they have the form

$$\psi^{(L)}(\mathbf{k},\mathbf{r}) = e^{i\mathbf{k}_\parallel\mathbf{r}_\parallel}\cdot\begin{cases} e^{ik_\perp z} + R\,e^{-ik_\perp z}, & z < -a/2, \\ T\,e^{ik_\perp z}, & z > a/2, \end{cases} \tag{43}$$

$$\psi^{(R)}(\mathbf{k},\mathbf{r}) = e^{i\mathbf{k}_\parallel\mathbf{r}_\parallel}\cdot\begin{cases} T\,e^{-ik_\perp z}, & z < -a/2, \\ e^{-ik_\perp z} + R\,e^{ik_\perp z}, & z > a/2. \end{cases} \tag{44}$$

In both cases $k_\perp \equiv |\mathbf{k}_\perp| > 0$ is the normal component of the neutron momentum, and $\mathbf{k}_\parallel$ is its component along the target surface.

The functions inside the layer, determined by the boundary conditions, can be written (for constant U) as

$$\psi^{(L,R)}(\mathbf{k},\nu) = e^{i\mathbf{k}_\parallel\mathbf{r}_\parallel}e^{-ik_\perp a/2} \times\frac{t\gamma^{1/2}}{1-r^2\gamma^2}\sum_{\sigma=\pm1}A_\sigma^{(L,R)}e^{i\sigma\bar{k}z}. \tag{45}$$

Here $\bar{k}$ is the normal component of neutron momentum inside the target sample

$$\bar{k} = \sqrt{k_\perp^2 - k_0^2}, \qquad k_0^2 = 4\pi\beta_c n, \tag{46}$$

where k_0 is the value of the neutron wave number $k_\perp$ at the barrier, r and t are the reflection and transition coefficients for the target surface

$$t = \frac{2k_\perp}{k_\perp+\bar{k}}, \qquad r = \frac{k_\perp-\bar{k}}{k_\perp+\bar{k}}, \tag{47}$$

and the coefficients A are determined by

$$A_{+1}^{(L)} = 1, \quad A_{-1}^{(L)} = -r\gamma, \quad A_{+1}^{(R)} = -r\gamma, \quad A_{-1}^{(R)} = 1. \tag{48}$$

The factor

$$\gamma = e^{i\bar{k}a} \tag{49}$$

oscillates very rapidly as a function of $k_\perp$ above the barrier ($k_\perp > k_0$), and vanishes below the barrier ($k_\perp < k_0$).

Below we use the "left" solution (43) for the input channel function. Then, the output channels with the backward and forward scattering angles correspond to the "left", L, (43) and "right", R, (44) solutions, respectively. Inside the layer these solutions can be represented as

$$\bar{\psi}^{(L,R)}(\mathbf{k}',\nu) = e^{-i\mathbf{k}'_\parallel\mathbf{r}_\parallel}e^{-ik'_\perp a/2} \times\frac{t'\gamma'^{1/2}}{1-r'^2\gamma'^2}\sum_{\sigma=\pm1}A'^{(L,R)}_\sigma e^{i\sigma\bar{k}'z}. \tag{50}$$

All momenta and momentum-dependent quantities (46)-(49) for the output channel are denoted by primes: $k'_\perp$, $\bar{k}'$, t', r', A'_σ, γ'. They are interrelated by the same equations as that for the input channel.

Combining (45) and (50) we obtain for (7)

$$\mathbf{B}(\mathbf{q}) = i\beta_c tt'\frac{e^{-i(k_\perp+k'_\perp)a/2}}{(1-r^2\gamma^2)(1-r'^2\gamma'^2)}\,\Sigma_\parallel\boldsymbol{\Sigma}. \tag{51}$$

Here

$$\Sigma_{\parallel} = \sum_{\nu_{\parallel}} e^{i(\mathbf{Q}_{\parallel} - \mathbf{q}_{\parallel})\mathbf{r}_{\parallel}}, \qquad \mathbf{Q}_{\parallel} = \mathbf{k}_{\parallel} - \mathbf{k}'_{\parallel}, \tag{52}$$

and

$$\boldsymbol{\Sigma} = \sum_{\sigma,\sigma'} A_{\sigma} A'_{\sigma'} \left(\mathbf{Q}_{\parallel} + Q_{\perp}^{\sigma\sigma'} \mathbf{e}_z \right) \Sigma_{\perp}^{\sigma\sigma'}, \tag{53}$$

where

$$Q_{\perp}^{\sigma\sigma'} = \sigma \bar{k} + \sigma' \bar{k}', \qquad \Sigma_{\perp}^{\sigma\sigma'} = (\gamma\gamma')^{1/2} \sum_{\nu_{\perp}} e^{i(Q_{\perp}^{\sigma\sigma'} - q_{\perp})z}. \tag{54}$$

Summation over the nuclei on the plane parallel to the target surface gives

$$\Sigma_{\parallel} = (2\pi)^2 n_{\parallel} \sum_{\mathbf{G}_{\parallel}} \delta^{(2)}(\mathbf{Q}_{\parallel} - \mathbf{q}_{\parallel} - \mathbf{G}_{\parallel}), \tag{55}$$

where summation over the longitudinal reciprocal lattice vector $\mathbf{G}_{\parallel}$ arises for crystals, and $n_{\parallel}$ is the number of nuclei per the unit area of the fixed plane (z = const). Therefore, we have the equality

$$\mathbf{Q}_{\parallel} = \mathbf{q}_{\parallel} + \mathbf{G}_{\parallel} \tag{56}$$

for the longitudinal transferred momentum.

The cross-section (6) is proportional to the second power of the quantity $\Sigma_{\parallel}$. Then,

$$\left|\Sigma_{\parallel}\right|^2 = S(2\pi)^2 n_{\parallel}^2 \sum_{\mathbf{G}_{\parallel}} \delta^{(2)}(\mathbf{Q}_{\parallel} - \mathbf{q}_{\parallel} - \mathbf{G}_{\parallel}), \tag{57}$$

where S is the surface area of the sample.

For a non-crystalline substance we replace summation over nuclear planes by integration

$$\Sigma_{\perp}^{\sigma\sigma'} = (\gamma\gamma')^{1/2} n_{\perp} \int\limits_{-a/2}^{a/2} e^{i(Q_{\perp}^{\sigma\sigma'} - q_{\perp})z} \mathrm{d}z \tag{58}$$

and obtain

$$\Sigma_{\perp}^{\sigma\sigma'} = (\gamma\gamma')^{1/2} n_{\perp} \Delta(q_{\perp} - Q_{\perp}^{\sigma\sigma'}), \tag{59}$$

where

$$\Delta(x) = \frac{2\sin(xa/2)}{x}. \tag{60}$$

Here $n_{\perp}$ is the number of nuclear planes per the unit length along the z-axis ($n_{\parallel} n_{\perp} = n$). The function $\Delta(x)$ peaks sharply for small values of the argument.

For crystals the sum $\Sigma_{\perp}^{\sigma\sigma'}$ has additional peaks when $Q_{\perp}^{\sigma\sigma'} - q_{\perp}$ is close to the transverse reciprocal lattice vector $G_{\perp}$. In this case we take

$$\Sigma_{\perp}^{\sigma\sigma'} = (\gamma\gamma')^{1/2} n_{\perp} \Delta(q_{\perp} + G_{\perp} - Q_{\perp}^{\sigma\sigma'}), \tag{61}$$

assuming that the argument in the Δ-function is in the first Brillouin zone. Since the vector $q_{\perp}$ (originated from correlation function) is in the first Brillouin zone, the vector $G_{\perp}$ should compensate, if necessary, the exceeding part of $Q_{\perp}^{\sigma\sigma'}$.

5 General expression for inelastic transition probability

With the given correlation function (41) and quantity $\mathbf{B}$ (51), the general expression for the inelastic cross-section (6) is fully defined and we can easily integrate over $\mathbf{q}_{\parallel}$ with the help of (57). Taking into account contributions from both longitudinal and transverse parts of the correlation function, we find

$$\frac{\mathrm{d}\sigma_{ie}^{l,t}}{\mathrm{d}^3 k'} = S \frac{\alpha n \beta_c^2 \hbar^2 n_0(\omega)}{2\pi k m M c_{l,t}^2} |t|^2 |t'|^2 \sum_{\mathbf{G}_{\parallel}} \Pi_{l,t}\,, \tag{62}$$

where the function

$$\Pi_{l,t} = \frac{|\gamma|\,|\gamma'|}{|1 - r^2\gamma^2|^2\,|1 - r'^2\gamma'^2|^2} \times \sum_{\sigma,\sigma',\tau,\tau'} A_{\sigma} A_{\tau}^{*} A'_{\sigma'} A'^{*}_{\tau'}\, J_{l,t}(\lambda,\eta) \tag{63}$$

includes all factors γ and γ' that are strongly oscillating above the barrier and exponentially small below it.

The factor $J_{l,t}(\lambda,\eta)$ depends on transverse momenta inside the target in combinations

$$\lambda = Q_{\perp}^{\sigma\sigma'} - G_{\lambda}, \qquad \eta = Q_{\perp}^{\tau\tau'^{*}} - G_{\eta}, \tag{64}$$

where λ and η are assumed to be in the first Brillouin zone, and the difference from the full combinations $Q_{\perp}^{\sigma\sigma'}$ and $Q_{\perp}^{\tau\tau'^{*}}$ (see (54)) is compensated by the transverse components G_{λ} and G_{η} of the reciprocal lattice vectors. The factor $J_{l,t}(\lambda,\eta)$ is defined by the integral with the correlation function $\Omega_{l,t}$ and has a different form for the longitudinal and transverse cases,

$$J_{l,t}(\lambda,\eta) = \frac{1}{\pi} \int\limits_{-\infty}^{+\infty} \mathrm{d}q_{\perp} \bar{\Omega}_{l,t}(q_{\perp}) \Delta(q_{\perp} - \lambda) \Delta(q_{\perp} - \eta) F_{l,t}(q_{\perp}), \tag{65}$$

where

$$F_l(q_{\perp}) = \frac{(\mathbf{Q}_{\parallel}\mathbf{q}_{\parallel} + Q_{\perp}^{\sigma\sigma'} q_{\perp})(\mathbf{Q}_{\parallel}\mathbf{q}_{\parallel} + Q_{\perp}^{\tau\tau'^{*}} q_{\perp})}{q_{\parallel}^2 + q_{\perp}^2}, \tag{66}$$

$$F_t(q_{\perp}) = Q_{\parallel}^2 + Q_{\perp}^{\sigma\sigma'} Q_{\perp}^{\tau\tau'^{*}} - F_l(q_{\perp}). \tag{67}$$

Note that the functions $F_{l,t}(q_{\perp})$, as well as $J_{l,t}$, depend on the indices σ, σ', τ and τ', but, to simplify notations, we omit them. Here and below we use $\mathbf{q}_{\parallel}$, defined from (56)

$$\mathbf{q}_{\parallel} = \mathbf{Q}_{\parallel} - \mathbf{G}_{\parallel}, \tag{68}$$

as a fixed quantity. The correlation function $\bar{\Omega}(q_{\perp})$, when parameterized as in (41) by Γ^2 and p^2, has a universal form for the longitudinal and transverse cases, and their specificity arises only from the numerical values of these parameters. Hence we shall omit the subscripts on $\bar{\Omega}(q_{\perp})$ till the last, numerical stage.

The inelastic transition probability (8) with the use of (62) takes the form

$$\frac{\mathrm{d}w_{l,t}(k_\perp, k_\parallel \to \varepsilon')}{\mathrm{d}\varepsilon'} = \frac{\alpha\beta_c k\, n_0(\omega)}{Mc_{l,t}^2}\, W_{l,t}(k_\perp, k_\parallel \to \varepsilon'), \tag{69}$$

where the dimensionless factor W is given by

$$W_{l,t}(k_\perp, k_\parallel \to \varepsilon') = \frac{k_\perp}{\pi^2 k}\int\limits_0^{k'} \mathrm{d}k'_\perp \int\limits_0^{\pi} \mathrm{d}\varphi\, |t'|^2\, \Pi_{l,t}. \tag{70}$$

Here one integrates over $k'_\perp$ (up to $k' = \sqrt{2m\varepsilon'}/\hbar$) and φ, the angle between $\mathbf{k}'_\parallel$ and $\mathbf{k}_\parallel$, with fixed ε'.

For crystals, the final momentum $\mathbf{k}'$ is split by parts inside the first Brillouin zone, $\mathbf{k}'_1$, and $\mathbf{G}$. So the integral (8) over $\mathbf{k}'$ should be understood as that over $\mathbf{k}'_1$ and, if necessary, as a sum over $\mathbf{G}$.

The detailed energy distribution inside a high Brillouin zone is of no interest, and we shall consider the full integrals over each zone, assuming that the final energy depends only on $\mathbf{G}$, $\varepsilon' \simeq \hbar^2 G^2/2m$. In analogy with (8), (69) and (70) we define the transition probability per bounce

$$w_{l,t}(k_\perp, k_\parallel \to \mathbf{G}) = \frac{1}{S_\perp}\int \frac{\mathrm{d}\sigma_{ie}^{l,t}}{\mathrm{d}^3 k'}\mathrm{d}^3 k', \tag{71}$$

which can be presented in the form

$$w_{l,t}(k_\perp, k_\parallel \to \mathbf{G}) = \frac{\alpha\beta_c k\, n_0(\hbar G^2/2m)}{Mc_{l,t}^2} \times \frac{\hbar^2 G^2}{2m}\, W_{l,t}(k_\perp, k_\parallel \to \mathbf{G}), \tag{72}$$

where

$$W_{l,t}(k_\perp, k_\parallel \to \mathbf{G}) = \frac{k_\perp}{\pi^2 k G^2}\int \mathrm{d}^3 k'\, \Pi_{l,t}(\mathbf{G}) \tag{73}$$

is the dimensionless factor.

The transition probabilities (69) and (72) are quite general and fully defined but rather complicated even for numerical analysis. However, a drastic simplification can be achieved by analytic calculations even for the general case.

In our present publication we consider only a specific case that is when the initial neutron energy is below the optical potential. Moreover, for the sake of simplicity, in the main part of the paper we shall use only the results of the theoretical calculations referring to the appendices where the calculations are presented in detail. Below we explain just the main steps of the solution.

First, in appendix A.1 we calculate the integral (65). It turns out to be performed "almost exactly" by transforming (65) into a contour integral in the complex $q_\perp$ plane with the use of the four-pole structure of the correlation function (41).

The next step, the calculation of the sum in (63), is performed in appendix A.2. Comparative importance of the 16 terms in the sum is very sensitive to the position of the initial and the final neutron energies. The result was obtained for the initial neutron energy below the barrier and for any final energy of the scattered neutron. After this stage, the inelastic cross-section is defined as a function of final neutron momentum, $\mathbf{k}'$.

The last stage, the integration over angular distribution of the scattered neutrons, is done in appendices A.3 and A.4. Here the momentum transfer between the neutron and crystal lattice is very specific and has required a quite different approach (see A.4).

We write down the final results for the dimensionless quantities (70) and (73).

For transitions inside the first Brillouin zone ($\mathbf{G} = 0$) the factor (70) was found as

$$W_l(k_\perp, k_\parallel \to \varepsilon') = \frac{k_\perp f(k'_\perp) x_0}{3\pi k} + \frac{2k_\perp \Gamma^2 k'^2}{\pi k \mathrm{æ}\left(k'^2 - \epsilon\,\omega^2/c_l^2\right)^{3/2}}, \tag{74}$$

$$W_t(k_\perp, k_\parallel \to \varepsilon') = \frac{2k_\perp f(k'_\perp) x_0}{3\pi k}, \tag{75}$$

where

$$f(k'_\perp) = \begin{cases} 4k'_\perp/k_0^2, & k'_\perp < k_0, \\ 4/(k'_\perp + \sqrt{k'^2_\perp - k_0^2}), & k'_\perp > k_0, \end{cases} \tag{76}$$

with $k'_\perp = \sqrt{k'^2 - k_\parallel^2}$,

$$\mathrm{æ} = \sqrt{k_0^2 - k_\perp^2}, \tag{77}$$

and

$$x_0(\omega) = \sqrt{\frac{\sqrt{(\epsilon\,\omega^2/c^2)^2 + \Gamma^4} + \epsilon\,\omega^2/c^2}{2}}. \tag{78}$$

The factors (73) for the case $\mathbf{G} \neq 0$ were reduced to

$$W_l(k_\perp, k_\parallel \to \mathbf{G}) = \frac{4k_\perp x_0}{3k\mathrm{æ}}, \tag{79}$$

$$W_t(k_\perp, k_\parallel \to \mathbf{G}) = \frac{8k_\perp x_0}{3k\mathrm{æ}}. \tag{80}$$

The transition probabilities (74), (75) and (79), (80) can be further simplified by averaging over the neutron incident angle. There are two factors with angular dependence in (74), (75) and (79), namely $k_\perp/(k\,\mathrm{æ})$ and $k_\perp f(k'_\perp)/k$. Following (16) we introduce

$$\left\langle \frac{k_\perp}{k\mathrm{æ}} \right\rangle = \frac{1}{4k} A\left(\frac{\varepsilon}{U}\right), \tag{81}$$

where

$$A(x) = \frac{1}{x}\left(\arcsin\sqrt{x} - \sqrt{x(1-x)}\right), \tag{82}$$

and

$$\left\langle \frac{k_\perp f(k'_\perp)}{k} \right\rangle = \frac{1}{k}\, B\left(\frac{\varepsilon}{U}, \frac{\varepsilon'}{U}\right), \tag{83}$$

where the function $B(x,x')$ has a different form in three regions of the variables: $x' < 1$, $1 < x' < 1+x$, $1+x < x'$, and can be presented as

$$B(x,x') = C\left(x, \frac{x'}{x}\right) - C\left(x, \frac{x'-1}{x}\right), \tag{84}$$

with

$$C(x,y) = x \int\limits_{\min(0,y)}^{\min(1,y)} \sqrt{(1-z)(y-z)}\, \mathrm{d}z. \tag{85}$$

Note the two simple limits

$$\begin{aligned} &B(x,x') \simeq x/2, && \text{for} \quad |x'-x| \ll 1, \\ &B(x,x') \simeq (1/3)\sqrt{x/x'}, && \text{for} \quad x' \gg 1. \end{aligned} \tag{86}$$

The final expressions for $W_{l,t}$, defined in (70) and (73), averaged over the angle of incidence, are of the form

$$W_l(\varepsilon \to \varepsilon') = \frac{x_0}{3\pi k}\, B\left(\frac{\varepsilon}{U}, \frac{\varepsilon'}{U}\right) + \frac{\Gamma^2 k'^2}{2\pi k \left(k'^2 - \epsilon\, \omega^2/c_l^2\right)^{3/2}}\, A\left(\frac{\varepsilon}{U}\right), \tag{87}$$

$$W_t(\varepsilon \to \varepsilon') = \frac{2x_0}{3\pi k} B\left(\frac{\varepsilon}{U}, \frac{\varepsilon'}{U}\right), \tag{88}$$

$$W_l(\varepsilon \to \mathbf{G}) = \frac{x_0}{3k} A\left(\frac{\varepsilon}{U}\right), \quad W_t(\varepsilon \to \mathbf{G}) = \frac{2x_0}{3k} A\left(\frac{\varepsilon}{U}\right). \tag{89}$$

The second terms both in (74) and (87) are valid only for large energy transfer (see eqs. (A.80), (A.81) and text before).

6 Application to inelastic scattering on solid and liquid target samples

In the previous section, specific cases of general equations were analyzed with the use of mathematical criteria. In this section, we consider the problems from a physical point of view, making classifications by the relaxation processes, phonon-like or diffusion-like types, and by the range of the energy transfer, with a special attention to the region of small heating and cooling, as well as to the upscattering region. The substances under investigation are of crystalline, amorphous and liquid type, commonly used in experiments.

There are two longitudinal modes, phonon-like and thermo-diffusion, for both solids and liquids, and only one transverse mode. The latter is of pure phonon type for solids, and of combined type for liquids, and transforms from diffusion type at small energy transfer to phonon type at large energy transfer (see sect. 3).

6.1 Phonon-like mode, G = 0

Phonon-like modes involve low damping, *i.e.* $\Gamma_p \to 0$. Therefore, one can neglect the last term in (87) and use for (78) $x_0(\omega) = |\omega|/c$. For solids, when $\mathbf{G} = 0$, the sum over longitudinal and transverse modes gives from (87) and (88)

$$\frac{\mathrm{d}w_p(\varepsilon \to \varepsilon')}{\mathrm{d}\varepsilon'} = \frac{\beta_c |\omega| n_0(\omega)}{\pi M c^3}\, B\left(\frac{\varepsilon}{U}, \frac{\varepsilon'}{U}\right), \tag{90}$$

where c is defined by

$$\frac{3}{c^3} = \frac{1}{c_l^3} + \frac{2}{c_t^3}. \tag{91}$$

For the low-energy part of the spectrum one can use (23) and find

$$\frac{\mathrm{d}w_p(\varepsilon \to \varepsilon')}{\mathrm{d}\varepsilon'} = \frac{\beta_c k_T v_T}{2\pi M c^3}\, B\left(\frac{\varepsilon}{U}, \frac{\varepsilon'}{U}\right), \quad |\varepsilon' - \varepsilon| \ll T. \tag{92}$$

This part of the spectrum is completely determined by the function $B(x,x')$. Here and below we use the quantities

$$k_T = \frac{\sqrt{2mT}}{\hbar}, \qquad v_T = \sqrt{\frac{2T}{m}}. \tag{93}$$

The contribution of inelastic processes with $\mathbf{G} = 0$ to the total probability of the UCN escape from the trap can be estimated by integration of (90) from the barrier U up to the Debye energy

$$\varepsilon_D = \hbar c (6\pi^2 n)^{1/3}. \tag{94}$$

Since $U \ll \varepsilon_D$, it gives

$$w_p(\varepsilon) = c_1\left(\frac{\varepsilon_D}{T}\right) \frac{\beta_c k_T}{12\pi} \frac{m}{M} \frac{v v_T^2}{c^3}, \tag{95}$$

where $v = \sqrt{2\varepsilon/m}$ is the initial neutron velocity, and

$$c_1(y) = \int\limits_0^y \frac{x^{1/2}\mathrm{d}x}{e^x - 1} \underset{y\to\infty}{\longrightarrow} 2.315. \tag{96}$$

For liquids, the contribution of the longitudinal phonon-like mode is of the form (90), (92) and (95), where $1/c^3$ should be replaced by $1/3c_l^3$. The transverse mode for liquids is considered below (see sect. 6.4).

6.2 Phonon upscattering, G ≠ 0

The main process for upscattering in crystals goes with momentum transfer from the lattice. Assuming $\Gamma_p \to 0$ and summing over longitudinal and transverse phonons, we obtain for the total upscattering probability from (72) and (89)

$$w_p^{up}(\varepsilon) = \frac{\beta_c \hbar^3}{4m^2 M c^3}\, A\left(\frac{\varepsilon}{U}\right) \sum_{\mathbf{G}_\parallel, G_\perp > 0} G^4 n_0\left(\frac{\hbar G^2}{2m}\right), \tag{97}$$

where c is given by (91). Restriction in the sum with $G_\perp > 0$ is made since the summation over backward and forward scattering was performed earlier.

To estimate the probability we replace summation over $G_\perp > 0$ and $\mathbf{G}_\parallel$ by integration

$$\sum_{\mathbf{G}_\parallel, G_\perp > 0} \quad \longrightarrow \quad \frac{1}{2}\int \frac{\mathrm{d}^3 G}{(2\pi/a_0)^3}, \tag{98}$$

where $a_0 = \sqrt[3]{M/\rho}$ is the lattice constant. The integral over $\varepsilon' = \hbar^2 G^2/2m$ up to the Debye energy gives

$$w_p^{up}(\varepsilon) = c_2\left(\frac{\varepsilon_D}{T}\right)\frac{\pi\beta_c k_T}{4}\left(\frac{a_0 k_T}{2\pi}\right)^3\frac{m}{M}\left(\frac{v_T}{c}\right)^3 A\left(\frac{\varepsilon}{U}\right), \tag{99}$$

where

$$c_2(y) = \int_0^y \frac{x^{5/2}\mathrm{d}x}{e^x - 1} \underset{y\to\infty}{\longrightarrow} 3.745. \tag{100}$$

The high-energy upscattering due to phonons at $\mathbf{G} \neq 0$, was considered earlier [14,15] by other approaches. The probability (99) coincides with the result, presented, for example, in the review paper [17].

6.3 Longitudinal thermo-diffusion mode, G = 0

The differential probability of inelastic scattering via this mode, which follows from (69) and (87) with $\epsilon = 0$, can be presented in the form

$$\frac{\mathrm{d}w_d(\varepsilon\to\varepsilon')}{\mathrm{d}\varepsilon'} = \frac{\alpha\beta_c\Gamma_d n_0(\omega)}{3\sqrt{2}\,\pi M c_l^2}\left(B\left(\frac{\varepsilon}{U},\frac{\varepsilon'}{U}\right) + \frac{3\hbar\Gamma_d}{2\sqrt{m\varepsilon'}}A\left(\frac{\varepsilon}{U}\right)\theta(\varepsilon'-\varepsilon)\left(1-e^{-\varepsilon'/10\varepsilon}\right)\right), \tag{101}$$

where the last term in (87), valid only for large energy transfer ($\varepsilon' \gg \varepsilon$), is written with factors $\theta(\varepsilon'-\varepsilon)$ and $(1-e^{-\varepsilon'/10\varepsilon})$, which provide attenuation at small ε' ($\theta(x) = 0$ for $x < 0$ and $\theta(x) = 1$ for $x > 0$). The damping parameter, Γ_d^2, given in (34), can be presented as

$$\frac{\Gamma_d}{k} = \left(\frac{|\varepsilon'-\varepsilon|}{d_D\varepsilon}\right)^{1/2}, \tag{102}$$

where

$$d_D = \frac{2mD_S}{\hbar} \tag{103}$$

is the dimensionless thermo-diffusion coefficient.

For small energy transfer, $\varepsilon' \sim \varepsilon$, the dominating first term in (101) takes the form

$$\frac{\mathrm{d}w_d(\varepsilon\to\varepsilon')}{\mathrm{d}\varepsilon'} \simeq \frac{\alpha\beta_c k_T}{6\pi M c_l^2}\frac{vv_T}{v_0^2\sqrt{2d_D}}\sqrt{\frac{\varepsilon}{|\varepsilon'-\varepsilon|}}, \tag{104}$$

where $v_0 = \sqrt{2U/m}$ is the barrier velocity. It is clear that the divergence at $\varepsilon' \to \varepsilon$ is integrable. This result for longitudinal thermo-diffusion and for fixed components $k_\perp$ and $k_\parallel$ of the initial neutron momentum was obtained in [13].

For large energy transfer, the main contribution comes from the second term in (101). It should be remembered that diffusion modes appear in hydrodynamic approximation. So, the energy transfer via this mode has sense only inside the hydrodynamic region (31), where $|\omega| \ll c_l^2/D_S$. It gives the boundary for ε', where (101) is reasonable,

$$\varepsilon' \ll \varepsilon_d \equiv \frac{2mc_l^2}{d_D}. \tag{105}$$

If $\varepsilon_D < \varepsilon_d$, the integration can be performed up to the Debye energy. It gives

$$w_d(\varepsilon) = c_1\left(\frac{\varepsilon_D}{T}\right)\frac{\alpha\beta_c k_T}{4\pi d_D}\frac{m}{M}\left(\frac{v_T}{c_l}\right)^2 A\left(\frac{\varepsilon}{U}\right). \tag{106}$$

6.4 Transverse mode for liquids, G = 0

Taking $\alpha = \epsilon = 1$ (see text after (41)), we get from (69) and (88) the differential probability of inelastic scattering

$$\frac{\mathrm{d}w_t(\varepsilon\to\varepsilon')}{\mathrm{d}\varepsilon'} = \frac{2\beta_c x_0(\omega) n_0(\omega)}{3\pi M c_t^2}\,B\left(\frac{\varepsilon}{U},\frac{\varepsilon'}{U}\right), \tag{107}$$

where $x_0(\omega)$ is given by (78) with $c \to c_t$, while the damping factor $\Gamma^2 \to \Gamma_t^2$ is of the form (37).

The hydrodynamic region (38), $|\omega| \ll c_t^2/\nu$, corresponds to the final neutron energy

$$\varepsilon' \ll \varepsilon_\nu \equiv \frac{2mc_t^2}{d_\nu}, \tag{108}$$

where

$$d_\nu = \frac{2m\nu}{\hbar} \tag{109}$$

is the dimensionless viscosity. On the other hand, (108) means $\Gamma_t^2 = |\omega|/\nu \gg \omega^2/c_t^2$, which simplifies $x_0(\omega)$,

$$x_0(\omega) = \frac{\Gamma_t}{\sqrt{2}}. \tag{110}$$

In the region $\varepsilon' \sim \varepsilon$, (107) takes the form

$$\frac{\mathrm{d}w_t(\varepsilon\to\varepsilon')}{\mathrm{d}\varepsilon'} \simeq \frac{\beta_c k_T}{3\pi M c_t^2}\frac{vv_T}{v_0^2\sqrt{2d_\nu}}\sqrt{\frac{\varepsilon}{|\varepsilon'-\varepsilon|}}, \tag{111}$$

similar to (104) for longitudinal thermo-diffusion.

Beyond the hydrodynamic region, *i.e.* for large energy transfer, we have

$$\Gamma_t^2 \ll \frac{\omega^2}{c_t^2} \quad \Longrightarrow \quad x_0(\omega) = \frac{|\omega|}{c_t}, \tag{112}$$

and (107) transforms into (90) for the transverse phonon-like mode, where $1/c^3$ should be replaced by $2/3c_t^3$.

6.5 Relative contribution of phonons and thermo-diffusion to large energy transfer

Phonon contribution to large energy transfer essentially depends on the momentum exchange with the lattice. The probability for upscattering with ($\mathbf{G} \neq 0$, eq. (99)) and without ($\mathbf{G} = 0$, eq. (95)) such exchange differs by the factor v/c ($\sim 10^{-3}$ for UCN). The physical reason is simple. Inelastic scattering can be visualized as an absorption by the neutron of a quantum from a medium with energy $\hbar\omega$ and momentum $\hbar q$. The requirement for energy and momentum conservation does not allow this process with "free" quanta. But for UCN the normal component of momentum is pure imaginary, $i\text{æ}$, and instead of a δ-function, as in (55) for $\mathbf{q}_\parallel$, one has from (58)-(60) for $q_\perp$

$$\Sigma_\perp^{1\sigma'} \sim \frac{e^{i(q_\perp + G_\perp - \sigma'\bar{k}')a/2}}{\text{æ} + i(q_\perp + G_\perp - \sigma'\bar{k}')}. \qquad (113)$$

Integrals over $q_\perp$ with (113) are very sensitive to the minimum value of the imaginary factor, $q_\perp + G_\perp - \sigma'\bar{k}'$, which may be reached in the allowed $q_\perp$ range. For sound-like excitations, a rough estimate gives

$$q = \frac{\omega}{c} \sim \frac{v'}{c}\, k' \ll k', \qquad (114)$$

where v' and k' are the velocity and the wave number of the scattered neutron. It is evident that the large factor $\sigma' k'$ in the denominator of (113) can be compensated only by $G_\perp$. Then (113) can result in the large factor $1/\text{æ}$, which is seen in (79), (80). With $G_\perp = 0$ one may expect, instead of $1/\text{æ}$, the factor $1/k'_\perp$, a result at least by factor v/c smaller.

Note that the factor $1/\text{æ}$ is of the scale of the UCN intrusion length into the wall of the trap. Therefore, it is natural that the inelastic-scattering probability is proportional to $1/\text{æ}$. Thus, the factor $1/k'_\perp$ instead of $1/\text{æ}$ points to the substantial suppression of the large energy transfer by the phonon mode with $\mathbf{G} = 0$.

The thermo-diffusion mode can be also effective for the large energy transfer, but the physics is quite different. The parameters ω and q of "diffusion quanta" are not strongly coupled, as in the phonon case, (114). Even with ω fixed by the energy transfer, $q_\perp$ is still allowed to be varied up to $\sim k'$. Thus, (113) can reach $1/\text{æ}$ even for $\mathbf{G} = 0$. The result can be seen from the last term in (74). It vanishes in the limit $\Gamma \to 0$ (for phonons), but is proportional to $1/\text{æ}$ for thermo-diffusion and results in the probability for upscattering (106) which may be comparable to that for phonons with $\mathbf{G} \neq 0$, (99).

7 Results for two specific target samples

In the previous section we have obtained analytic results for each type of relaxation modes. To get the physical result for a specific experiment, one should combine several analytic formulae with the relaxation modes and parameters appropriately chosen. To demonstrate this procedure and examine general trends of final results and their sensitivity to physical parameters, it is worthwhile to consider some specific examples.

We have chosen stainless steel (SS) and Fomblin fluid (FF), two materials which are often used in real experiments and, on the other hand, have quite different relaxation properties. Both materials are not of a simple structure, and we shall use for them simplified descriptions, which are specified below.

7.1 Parameters for stainless steel

The nuclei ^{56}Fe are the dominant ones in stainless steel. Thus, we take $A = 56$, where $A = M/m$ is the mass number of the scatterer. Then, $\rho = 7.8$ g/cm^3 and, therefore, $n = 8.4 \cdot 10^{22}$ cm^{-3} and $a_0 = 2.3 \cdot 10^{-8}$ cm. For the coherent-scattering length we take $b_c = 0.87 \cdot 10^{-12}$ cm, which gives for the barrier energy $U = 192$ neV. Sound velocities at $T = 293$ K are equal to $c_l = 5850$ m/s and $c_t = 3230$ m/s.

For the case of stainless steel one should consider contributions from longitudinal and transverse phonons and thermo-diffusion, the main part of the diffusion-like processes. For the latter, we need $\alpha = C_P/C_V - 1$ and the thermo-diffusion coefficient D_S,

$$\alpha = \frac{TK\beta_P^2}{\rho C_P}, \qquad D_S = \frac{\text{æ}}{\rho C_P}, \qquad (115)$$

where $K = -V(\partial P/\partial V)$ is the volume elasticity, and $\beta_P = (\partial V/\partial T)_P/V$ is the thermal coefficient of volume expansion. The corresponding values at normal temperature $T = 293$ K are listed in table 1 as well as the calculated quantities α, D_S, and dimensionless parameters d_D and d_ν.

7.2 Parameters for Fomblin fluid

Fomblin is a hydrogen-free fluorinated oil (it is known also as perfluropolyether). It is quite viscous at room temperature and used to cover the walls of UCN storage traps because of the small neutron absorption and upscattering rate. There are different modifications of Fomblin oil and not all of them are described in the literature in detail. Thus, we use typical values for Fomblin parameters. In addition, we ignore the complex structure of Fomblin molecules and we are treating it as a simple liquid.

The stoichiometry is roughly C_3F_6O. All nuclei entering the oil scatter the neutron; we take the mass number, $A = 16$, of dominating ^{16}F nuclei as the mass number of a "typical" scatterer. The Fomblin density is $\rho = 1.9$ g/cm^3, then $n = 7.15 \cdot 10^{22}$ cm^{-3}. For the coherent scattering length we use $b_c = 0.565 \cdot 10^{-12}$ cm, which gives $U = 106$ neV in accordance with experiment. For all temperatures we take fixed sound velocities: $c_l = 1900$ m/s and $c_t = 1500$ m/s.

The parameters K, β_P, C_P, æ, ν as well as the calculated α, D_S, and dimensionless quantities d_D and d_ν

Table 1. Parameters for stainless steel (SS) and Fomblin fluid (FF).

	T, K	K, Pa	β_P, K^{-1}	C_P, $\frac{\mathrm{J}}{\mathrm{g\,K}}$	æ, $\frac{\mathrm{W}}{\mathrm{m\,K}}$	ν, $\frac{\mathrm{cm}^2}{\mathrm{s}}$	α	D_S, $\frac{\mathrm{cm}^2}{\mathrm{s}}$	d_D	d_ν
SS	293	$170{\cdot}10^9$	$3.6{\cdot}10^{-5}$	0.45	80	0.01	0.018	$2.28{\cdot}10^{-1}$	717.5	31.5
FF	293	$3{\cdot}10^9$	$6{\cdot}10^{-4}$	1.0	0.2	1.40	0.167	$1.05{\cdot}10^{-3}$	3.30	4405.7
	373	$2{\cdot}10^9$	$7{\cdot}10^{-4}$	1.1	0.2	0.07	0.175	$0.96{\cdot}10^{-3}$	3.02	220.3

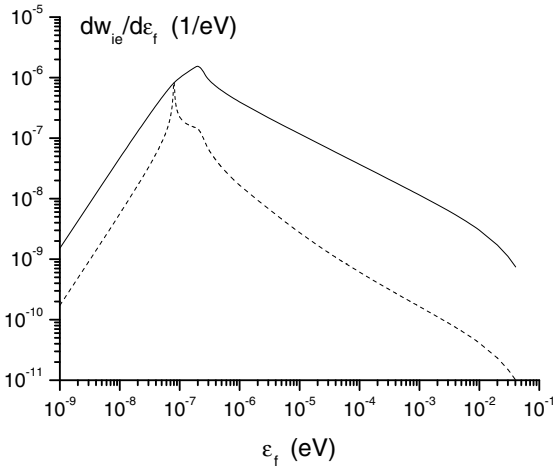

Fig. 1. Inelastic scattering for UCN of 80 neV on stainless steel at $T = 293$ K: the differential probability $\mathrm{d}w_{ie}/\mathrm{d}\varepsilon_f$ per bounce as a function of the final neutron energy ε_f. Solid line: phonon contribution, dashed line: thermo-diffusion contribution.

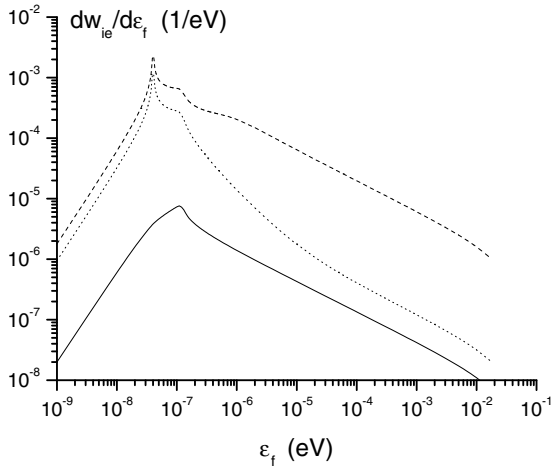

Fig. 2. Inelastic scattering for UCN of 40 neV on Fomblin oil at $T = 293$ K: the differential probability $\mathrm{d}w_{ie}/\mathrm{d}\varepsilon_f$ per bounce as a function of the final neutron energy ε_f. Solid line: longitudinal sound contribution, dotted line: transverse sound contribution, dashed line: thermo-diffusion contribution.

are presented in table 1 for two temperatures: $T = 293$ K and 373 K. Among these parameters, the viscosity ν is the most sensitive to the temperature.

7.3 Numerical results

We have calculated the probability of inelastic scattering for UCN with initial energy near half of the barrier height, that is for $\varepsilon = 80$ neV for stainless steel and $\varepsilon = 40$ neV for Fomblin. Contributions of phonons and diffusion modes are shown separately. Results for the differential probability are presented in figs. 1, 2 and 3.

Integral probabilities

$$w(\varepsilon_f) = \int_U^{\varepsilon_f} \frac{\mathrm{d}w(\varepsilon \to \varepsilon')}{\mathrm{d}\varepsilon'}\,\mathrm{d}\varepsilon' \qquad (116)$$

of transition to the interval $U < \varepsilon' < \varepsilon_f$ per bounce are shown in figs. 4, 5 and 6. For Fomblin both differential and integral inelastic-scattering probabilities are presented for two different temperatures: 293 K and 373 K.

Test calculations have been carried out starting from the exact expressions (69) and (70). The comparison with results from simplified analytic formulae has shown quite small deviations in the whole energy range. So, we present numerical results based on analytic formulae.

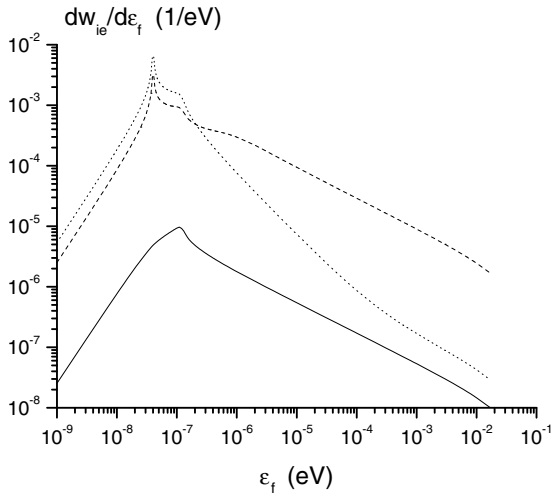

Fig. 3. Inelastic scattering for UCN of 40 neV on Fomblin oil at $T = 373$ K: the differential probability $\mathrm{d}w_{ie}/\mathrm{d}\varepsilon_f$ per bounce as a function of the final neutron energy ε_f. Solid line: longitudinal sound contribution, dotted line: transverse sound contribution, dashed line: thermo-diffusion contribution.

For stainless steel, the phonon contribution at $\mathbf{G} = 0$ was calculated from (90) and thermo-diffusion contribution from (101). Results at $T = 293$ K are shown by solid and dashed lines, respectively, in figs. 1 and 4. The final neutron energy for stainless steel is restricted from above by the Debye energy $\varepsilon_D = 0.040$ eV (A.71) with

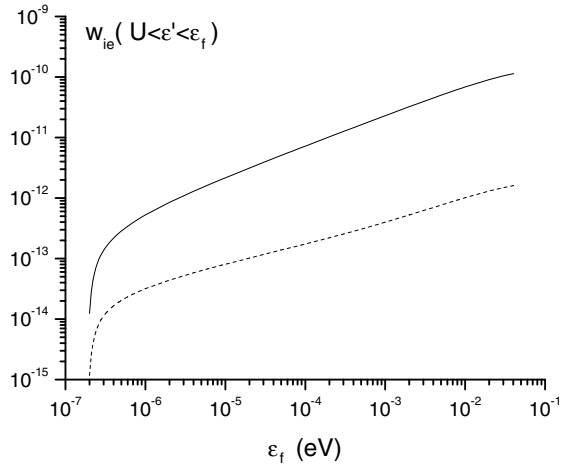

Fig. 4. Inelastic scattering for UCN of 80 neV on stainless steel at $T = 293$ K: the integral probability w_{ie} per bounce of transition to the interval $U < \varepsilon < \varepsilon_f$ as a function of ε_f. Solid line: phonon contribution, dashed line: thermo-diffusion contribution.

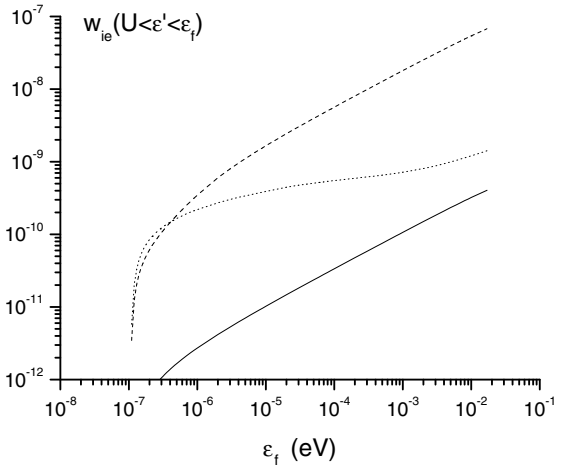

Fig. 6. Inelastic scattering for UCN of 40 neV on Fomblin oil at $T = 373$ K: the integral probability w_{ie} per bounce of transition to the interval $U < \varepsilon < \varepsilon_f$ as a function of ε_f. Solid line: longitudinal sound contribution, dotted line: transverse sound contribution, dashed line: thermo-diffusion contribution.

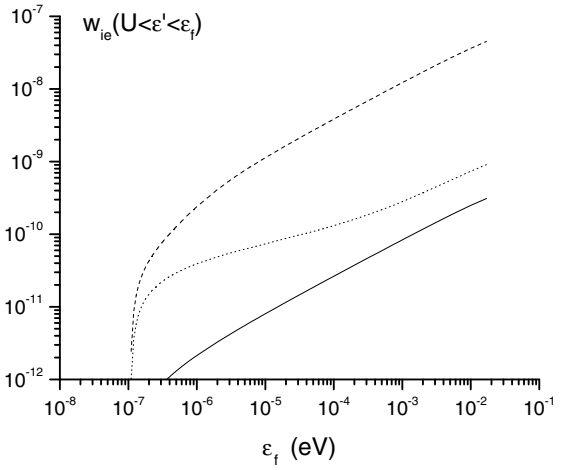

Fig. 5. Inelastic scattering for UCN of 40 neV on Fomblin oil at $T = 293$ K: the integral probability w_{ie} per bounce of transition to the interval $U < \varepsilon < \varepsilon_f$ as a function of ε_f. Solid line: longitudinal sound contribution, dotted line: transverse sound contribution, dashed line: thermo-diffusion contribution.

sound velocity c from (91). The thermo-diffusion contribution should be restricted from above by the limit energy $\varepsilon_d = 0.001$ eV (see (105)).

Integral probabilities in fig. 4, calculated for $\mathbf{G} = 0$, should be compared with the total upscattering probability at $\mathbf{G} \neq 0$, which is given by (99). At the temperature $T = 293$ K, it is equal to

$$w_p^{up} = 0.7 \cdot 10^{-6}. \tag{117}$$

For Fomblin, the longitudinal sound (phonon) contribution is given by (90) with $1/c^3 \to 1/3c_l^3$ (see the end of sect. 6.1), the transverse sound contribution by (107) and the thermo-diffusion contribution by (101). They were calculated both at $T = 293$ K and $T = 373$ K and are shown by solid, dotted and dashed lines, respectively, in figs. 2, 3, 5 and 6. The final neutron energy is restricted from above by the Debye energy $\varepsilon_D = 0.017$ eV (A.71) with sound velocity from (91). For Fomblin, the energy $\varepsilon_d = 0.023$ eV (105), the limit for thermo-diffusion contribution, is greater than the Debye energy ε_D.

8 Discussion

Differential spectra (figs. 1, 2 and 3) have well-developed maxima for both modes, phonon (with $\mathbf{G} = 0$) and diffusion-like. For the phonon mode, the peak shape is determined by the function $B(\varepsilon/U, \varepsilon'/U)$. It has a maximum at $\varepsilon' = U$ ($\varepsilon < U$). In diffusion-like modes there is a divergence (integrable) at $\varepsilon' \simeq \varepsilon$ (see (104) and (111)). These general forms of the curves are the same for stainless steel and Fomblin, but the relative contribution from phonon-like and diffusion-like modes are quite different for the two substances. Contributions from phonons and diffusion into small energy transfer can be estimated from (92) and (104), (111). Omitting numerical factors, one has for diffusion-to-phonon contribution ratio

$$\frac{w_d}{w_p} \sim \frac{\alpha c}{v_0 \sqrt{d}}. \tag{118}$$

For thermo-diffusion, the high value of the ratio c/v_0 may be compensated by the smallness of the quantity $\alpha = C_P/C_V - 1$ and additionally suppressed by the factor $1/\sqrt{d_D}$, when d_D is large. This is just the case for stainless steel, when the right part of (118) is near unity. As for Fomblin, the right-hand side of (118) is near 40. This qualitative estimate agrees with the numerical results presented in figs. 1, 2 and 3. The thermo-diffusion contribution is comparable with the phonon one for stainless steel (fig. 1) and dominates for Fomblin fluid (figs. 2 and 3).

The transverse relaxation mode in liquids for small energy transfer is also of diffusion type, which originates

from sound waves with high damping due to viscosity. The contribution of this mode, as compared to the longitudinal phonon one, can be evaluated from (118) with $\alpha = 1$. It far exceeds unity in agreement with figs. 2 and 3.

It should be emphasized that the two diffusive modes, which, due to the large ratio (118), give the main contribution to the small energy transfer for Fomblin, are governed by different physical parameters. The transverse mode has no small parameter α, but its quantity $d \to d_\nu$ (109) differs from that for thermo-diffusion, d_D (103), by magnitude and temperature dependence (see table 1).

Remark. The transverse mode was considered here with a simple liquid model (35)-(37), where transition to "ideal" liquid with very low viscosity is not correct. In this paper we have performed calculations for $d \geq 1$ (see sect. A.3.1), so the definition (109) gives the lower bound for the viscosity ν. (In [13] we have argued that for small $d < 1$ the contribution of the diffusion mode to inelastic scattering vanishes.)

Let us now discuss the quantitative results for the probability per bounce (116) for the neutron to change its energy from U up to $(10\text{–}10^3) \cdot U$, that is to go from the ultracold to the very cold energy region ("small heating"). For stainless steel, the probability for neutron transition to the region from U to $(10\text{–}10^3) \cdot U$ is of the scale of $\sim 10^{-13}$–10^{-11} (fig. 4), while for Fomblin it is of the scale of $\sim 10^{-10}$–10^{-9} (figs. 5 and 6). Evidently, these contributions could not be seen in the measurements [5–9].

As a general conclusion, phonons are ineffective for small energy transfer for both stainless steel and Fomblin. Thermo-diffusion is even less effective for stainless steel, but gives very large effect (one-two orders of magnitude larger than phonons) for Fomblin, where the transverse diffusion mode gives comparable contribution and even exceeds thermo-diffusion when the temperature goes up. (Note, however, that it goes down more steeply when the transferred energy becomes higher.)

In the region of high-energy transfer, the ratio of thermo-diffusion and phonon (at $\mathbf{G} = 0$) contributions can be estimated from (95) and (106),

$$\frac{w_d}{w_p} \sim \frac{\alpha c}{v_0 d_D}. \tag{119}$$

It is of the scale of 10^{-1} for stainless steel and 10^2 for Fomblin fluid. Thus, thermo-diffusion may dominate over phonons not only for small energy transfer, but also for a large one, provided the dimensionless thermo-diffusion coefficient d_D is low. This conclusion may have sense only for liquids and amorphous materials, since for crystals, and stainless steel in particular, the main process for the transition up to the temperature region, upscattering, is that characterized by momentum exchange with the lattice, $\mathbf{G} \neq 0$ (see sect. 6.5).

Therefore, the processes responsible for high-energy transfer are quite different for crystals and amorphous materials. Our result for coherent UCN upscattering on pure crystalline material (99) coincides with that previously obtained. It is known that its estimate (117) is one-two orders of magnitude too small to be observed in real storage experiments. The most probable reason is a much higher absorption rate due to the radiative capture and possible upscattering on hydrogen contamination of the surface.

For Fomblin only the surface effects have been discussed in detail so far. We have not found any published results with the evaluation of the escape probability from the bulk properties of this material. In other words, there is no understanding as to why the parameter f (see [23]) of bulk losses lies in the range from 10^{-5} to 10^{-6}. Thus our result just for bulk effect given by the integral (116) (calculated with $\varepsilon_f = \varepsilon_D$) is new. Numerical results for Fomblin presented in figs. 5 and 6 give for the loss probability per bounce ($\simeq f$) the following values: $0.5 \cdot 10^{-7}$ at 293 K and $0.7 \cdot 10^{-7}$ at 373 K. Possible reasons for the discrepancy of one-two orders of magnitude are mentioned in the conclusion.

9 Conclusion and outlook

A theory for coherent inelastic scattering of ultracold neutrons was developed with a quite general form of the correlation function, which allows to consider energy-momentum exchange of the neutron with sound waves (phonons) as well as with diffusion-like relaxations. The latter appear when a correlation function is considered in the hydrodynamic region of momentum and energy transfers (the low limit for $\mathbf{q}$ and ω). Namely, we discussed the longitudinal thermo-diffusion mode both for solids and liquids as well as the diffusion-like transverse mode for liquids.

In the frame of this theory, we evaluated the probability per bounce for an ultracold neutron to gain energy and to go into a cold or a thermal region. In this paper the case $\mathbf{G} = 0$ (*i.e.* no momentum transfer between the neutron and the crystal lattice) is consistently considered for the first time.

Numerical estimates are presented for the stainless-steel storage bottle and one with Fomblin-fluid–coated walls. For Fomblin, the most explored experimentally, theory predicts the overwhelming effect for thermo-diffusion processes, two-three orders of magnitude larger than from phonons, and a quite strong dependence on the temperature originated from viscosity.

However, the numerical values for the upscattering probability per bounce obtained for stainless steel as well as for Fomblin are still one-two orders of magnitude too small to fully explain experimental data. Thus, it is worthwhile to mention restrictions of the presented results and possible future improvements.

Results from diffusion processes are quite sensitive to the parameters of the correlation function. It is very desirable to clarify the structure and parameters of the correlation function, especially for liquids. In fact, it can be done by experiments in optics and other means outside the neutron physics.

We considered our samples as a spatially uniform medium. This may not be correct for Fomblin, which exhibits some polymer features and may have a non-uniform

structure at the scales comparable with the ultracold neutron reduced wavelength ~ 10 nm. To get the correlation function for the polymer and to include it in the neutron scattering theory is a serious problem for the future. Nevertheless, the effect may be evaluated from simple physical arguments. The probability for energy transfer, as was mentioned above, is proportional to the intrusion length or, what is the same, to the time of neutron-wall collision. The spatial polymer structure changes, in particular, the self-diffusion parameters for the neutron and increases the time spent by the neutron inside the sample during the collision. This time can be evaluated from transmission experiments and the corresponding correction can be easily introduced into the formulae of this paper.

On the other hand, gigantic polymer molecules can behave as nano-particles. If this is the case, the elastic scattering of the neutron by the whole moving molecule in their center-of-mass system would result in the inelastic scattering of the neutron in the laboratory system. A similar mechanism of small cooling and heating due to nano-particles at the surface of solid materials was proposed in [31].

Surface excitations, say, capillary waves, influence substantially the UCN losses from the traps with walls coated by Fomblin [23]. They can be included into consideration as one of the excitation modes. This particular case requires a different correlation function. By the same way, incoherent contributions of different nature seem important for a quantitative description of data on inelastic scattering of UCN. All these factors are subjects for separate studies.

We are kindly grateful to V.I. Morozov, E. Korobkina and R. Golub for valuable discussions. The work was supported by RFBR grant 02-02-16808, grant NS-1885.2003.2 and the program of bilateral cooperation between Russia and Germany, grant No. RUS 02/030.

Appendix A. Calculation of the inelastic cross-section and inelastic transition probability

The aim of this appendix is to simplify the general expression (62)-(63) for the inelastic cross-section. The first stage is the calculation of the integral (65).

Appendix A.1. Calculation of the integral $J_{l,t}(\lambda,\eta)$, eq. (65)

We start with a general integral of the form

$$I(\lambda,\eta)=\frac{1}{\pi}\int\limits_{-\infty}^{+\infty}\mathrm{d}q_\perp\,\Delta(q_\perp-\lambda)\Delta(q_\perp-\eta)\mathcal{F}(q_\perp),\quad (A.1)$$

where λ and η are complex parameters, and $\mathcal{F}(q_\perp)$ is a function with poles above ($q_{n\uparrow}$) and below ($q_{n\downarrow}$) the real axis, but not near it. The function $\Delta(x)$ is defined by (60), and therefore

$$\Delta(q_\perp-\lambda)\Delta(q_\perp-\eta)=\frac{1}{(q_\perp-\lambda)(q_\perp-\eta)}\times\left(2\cos\frac{(\lambda-\eta)a}{2}-e^{i\left(q_\perp-\frac{\lambda+\eta}{2}\right)a}-e^{-i\left(q_\perp-\frac{\lambda+\eta}{2}\right)a}\right).\quad (A.2)$$

We transform (A.1) into the contour integral closing a path in the upper or the lower half-plane. Then, neglecting the term proportional to $e^{-\mathrm{Im}\,q_{n\uparrow}a}$ and $e^{-|\mathrm{Im}\,q_{n\downarrow}|a}$, we get for any positions of λ and η

$$I(\lambda,\eta)=\frac{2\sin(\lambda-\eta)a/2}{\lambda-\eta}\left(\mathcal{F}(\lambda)+\mathcal{F}(\eta)\right)+\frac{2\cos(\lambda-\eta)a/2}{\lambda-\eta}\left(\mathcal{P}(\lambda)-\mathcal{P}(\eta)\right),\quad (A.3)$$

where the function $\mathcal{P}(\lambda)$ is defined by the residues in poles of $\mathcal{F}(q_\perp)$

$$\mathcal{P}(\lambda)=-i\left(\sum_{n\uparrow}\frac{\mathrm{res}_{n\uparrow}\mathcal{F}}{\lambda-q_{n\uparrow}}-\sum_{n\downarrow}\frac{\mathrm{res}_{n\downarrow}\mathcal{F}}{\lambda-q_{n\downarrow}}\right).\quad (A.4)$$

To apply the results for (65), one needs to specify the pole structure of the integrand. For the factors $F_{l,t}(q_\perp)$, it is evident from (66) and (67). The function $\bar{\Omega}_{l,t}(q_\perp)$ is given by (41) and can be presented as the sum of four simple pole terms. The poles are located symmetrically with respect to the axes at the points $x\pm iy$ and $-x\pm iy$, where

$$x=\sqrt{\frac{\sqrt{p^4+\Gamma^4}-p^2}{2}},\quad y=\sqrt{\frac{\sqrt{p^4+\Gamma^4}+p^2}{2}}\quad (A.5)$$

are real and positive. The function $\bar{\Omega}(q_\perp)$ takes the form

$$\bar{\Omega}(q_\perp)=\frac{1}{4i|z|^2}\left(U(q_\perp,z^*)-U(q_\perp,z)\right),\quad (A.6)$$

where $z=x+iy$ and

$$U(\alpha,z)=\frac{z}{\alpha-z^*}+\frac{z^*}{\alpha+z}.\quad (A.7)$$

This complex function of two complex variables will be extensively used below and it is worthwhile to exhibit its symmetry

$$U(\alpha,z)=U(-\alpha,-z)=-U(-\alpha,z^*)=U^*(\alpha^*,z^*).\quad (A.8)$$

The real and imaginary parts of this function for the first argument $\beta+i\gamma$ are of the form

$$\mathrm{Re}\,U(\beta+i\gamma,z)=\frac{2\beta x}{\Delta}\left(\beta^2+(\gamma+2y)^2-|z|^2\right),\quad (A.9)$$

$$\mathrm{Im}\, U(\beta+i\gamma,z) = -\frac{2x}{\Delta}\left(\beta^2\gamma + (\gamma+2y)(x^2+(\gamma+y)^2)\right), \tag{A.10}$$

where

$$\Delta = \left(\beta^2 + x^2 + (\gamma+y)^2\right)^2 - 4\beta^2 x^2. \tag{A.11}$$

Note that $U(i\gamma,z)$ is pure imaginary and given by

$$\mathrm{Im}\, U(i\gamma,z) = -\frac{2x(\gamma+2y)}{x^2+(\gamma+y)^2}. \tag{A.12}$$

Now, we are ready to apply the general result (A.3) and (A.4) to the integral (65). It is enough to find three "elementary" integrals $I_n(\lambda,\eta)$ $(n=1,2,3)$ with

$$\begin{aligned} \mathcal{F}_1(q_\perp) &= \bar{\Omega}(q_\perp), \\ \mathcal{F}_2(q_\perp) &= \frac{\bar{\Omega}(q_\perp)}{q_\parallel^2+q_\perp^2}, \\ \mathcal{F}_3(q_\perp) &= \frac{q_\perp\bar{\Omega}(q_\perp)}{q_\parallel^2+q_\perp^2}. \end{aligned} \tag{A.13}$$

All $\mathcal{F}_n(q_\perp)$ have the poles from $\bar{\Omega}(q_\perp)$, the last two have the additional poles in $q_\perp = \pm iq_\parallel$. The functions $\mathcal{P}_n(\lambda)$ take the form

$$\begin{aligned} \mathcal{P}_1(\lambda) &= -\frac{1}{4|z|^2}\left(U(\lambda,z^*)+U(\lambda,z)\right), \\ \mathcal{P}_2(\lambda) &= \frac{\mathcal{P}_1(\lambda)}{q_\parallel^2+\lambda^2} - \frac{i\lambda U(iq_\parallel,z)}{2q_\parallel|z|^2(q_\parallel^2+\lambda^2)}, \\ \mathcal{P}_3(\lambda) &= \frac{\lambda\mathcal{P}_1(\lambda)}{q_\parallel^2+\lambda^2} + \frac{iq_\parallel U(iq_\parallel,z)}{2|z|^2(q_\parallel^2+\lambda^2)}. \end{aligned} \tag{A.14}$$

Note that $\mathcal{F}_n$ and $\mathcal{P}_n$, which determine $I_n(\lambda,\eta)$ by (A.3), contain the function $U(\alpha,z)$ (A.7) varied by the first argument.

The function $J(\lambda,\eta)$ (65) can be presented as a sum of $I_n(\lambda,\eta)$ with coefficients evident from (66) and (67). After some rearrangement the results can be written in the form

$$J_{l,t}(\lambda,\eta) = J_{l,t}^{(1)}(\lambda,\eta) + J_{l,t}^{(2)}(\lambda,\eta). \tag{A.15}$$

Both terms in the right-hand side are proportional to the factors $U(\alpha,\beta)$, however, $J^{(1)}$ includes all terms with $\alpha = \lambda$ or η, while $J^{(2)}$ includes terms with $\alpha = iq_\parallel$. Namely,

$$J_{l,t}^{(1)}(\lambda,\eta) = \frac{e^{-i\frac{(\lambda-\eta)a}{2}}\Lambda_{l,t}(\lambda,\eta) - e^{i\frac{(\lambda-\eta)a}{2}}\Lambda_{l,t}(\eta,\lambda)}{\lambda-\eta}, \tag{A.16}$$

$$J_{l,t}^{(2)}(\lambda,\eta) = \cos\frac{(\lambda-\eta)a}{2}\,\Phi_{l,t}(\lambda,\eta)\,\frac{\mathrm{Im}\, U(iq_\parallel,z)}{q_\parallel|z|^2}, \tag{A.17}$$

where

$$\Lambda_{l,t}(\lambda,\eta) = -\frac{F_{l,t}(\lambda)U(\lambda,z) - F_{l,t}(\eta)U(\eta,z^*)}{2|z|^2}, \tag{A.18}$$

$$\begin{aligned} \Phi_{l,t}(\lambda,\eta) = \pm&\frac{1}{(q_\parallel^2+\lambda^2)(q_\parallel^2+\eta^2)} \\ &\times\Big(q_\parallel^2(\mathbf{Q}_\parallel\mathbf{q}_\parallel + \lambda Q_\perp^{\sigma\sigma'})(\mathbf{Q}_\parallel\mathbf{q}_\parallel + \eta Q_\perp^{\tau\tau'^*}) \\ &- Q_\perp^{\sigma\sigma'}q_\parallel^2)(\eta\mathbf{Q}_\parallel\mathbf{q}_\parallel - Q_\perp^{\tau\tau'^*}q_\parallel^2)\Big), \end{aligned} \tag{A.19}$$

and the functions $F_{l,t}$ are given by (66) and (67). In (A.19) "+" and "−" correspond to "l" and "t", respectively.

Note that the dependence on the parameter a, the thickness of the layer, is explicitly indicated in (A.16) and (A.17). All other functions are independent of a. The functions F and Φ are constructed entirely from kinematic factors, initial and final neutron momenta. The parameters of the correlation function, $z = x+iy$, apart from the explicit factor $|z|^2$, enter only in the function $U(\alpha,z)$ with $\alpha = \lambda,\eta$ or $iq_\parallel$.

The cross-section (62), (63) is the function of the incoming and outcoming neutron wave vectors, which are included in parameters $\mathbf{Q}_\parallel = \mathbf{k}_\parallel - \mathbf{k}'_\parallel$ (52) and $Q_\perp^{\sigma\sigma'}$, $Q_\perp^{\tau\tau'}$ (54). For the crystal these parameters are split into the parts inside the first Brillouin zone, $\mathbf{q}_\parallel$, λ, η, and corresponding reciprocal lattice vectors $\mathbf{G}_\parallel$, G_λ, G_η. Note that

$$F_l(\lambda) = F_l(\eta) = Q_\parallel^2 + Q_\perp^{\sigma\sigma'}Q_\perp^{\tau\tau'^*}, \tag{A.20}$$

$$F_t(\lambda) = F_t(\eta) = 0, \quad \Phi_{l,t}(\lambda,\eta) = \pm Q_\parallel^2, \tag{A.21}$$

when all $\mathbf{G}_\parallel$, G_λ, G_η are zero.

Thus, with calculated $J(\lambda,\eta)$, the general expression for the inelastic cross-section is of the form (62), (63) as the sum over the indices σ, σ', τ, τ'. This summation, for a general case, is cumbersome because the variables λ and η (64) enter the functions $U(\lambda,z)$ and $U(\eta,z)$ in a sophisticated way.

Appendix A.2. Inelastic cross-section for initial sub-barrier neutrons

In this appendix we specify the general expression for the inelastic cross-section (62), (63) for the case when the initial neutron is a sub-barrier. The final energy can be both below and above the barrier. The scheme of approximation varies for these two cases, and they will be considered separately. The object of analysis will be the factor $\Pi_{l,t}$ in the cross-section (62). All other factors are universal and will be added afterwards.

For the initial sub-barrier neutron it is useful to define

$$\bar{k} = i\text{æ}, \qquad \text{æ} = \sqrt{k_0^2 - k_\perp^2}. \tag{A.22}$$

The quantity $\gamma = e^{-\text{æ}a} \to 0$ for the initial channel may be neglected everywhere. In particular, for the neutron coming from the left we have

$$A_{+1}^{(L)} = 1, \qquad A_{-1}^{(L)} = -r\gamma \to 0. \tag{A.23}$$

To compensate γ in the first factor in (63) we need the second factor (the sum) be proportional to $\gamma^{-1} =$

$e^{æa}$. Therefore, the factor needed comes only from the first exponent in (A.16) with $\sigma = \tau = 1$. The same exponent should be taken into account in (A.17).

Following (A.15), the Π factor (63) can be presented as the sum of two terms

$$\Pi_{l,t}^{(1)} = \frac{|\gamma'|}{|1 - r'^2\gamma'^2|^2} \sum_{\sigma',\tau'} A'_{\sigma'} A'^*_{\tau'} \times (\gamma')^{-\sigma'/2} (\gamma'^*)^{-\tau'/2} \frac{\Lambda_{l,t}^{\sigma'\tau'}(\lambda,\eta)}{\lambda - \eta}, \quad \text{(A.24)}$$

$$\Pi_{l,t}^{(2)} = \frac{|\gamma'|}{|1 - r'^2\gamma'^2|^2} \frac{\operatorname{Im} U(iq_\parallel, z)}{2q_\parallel |z|^2} \sum_{\sigma',\tau'} A'_{\sigma'} A'^*_{\tau'} \times (\gamma')^{-\sigma'/2} (\gamma'^*)^{-\tau'/2} \Phi_{l,t}^{\sigma'\tau'}(\lambda,\eta). \quad \text{(A.25)}$$

The parameters λ and η are defined by (64) and can be rewritten now as

$$\lambda = i\text{æ} + \sigma'\bar{k}'_1, \qquad \eta = -i\text{æ} + \tau'\bar{k}'^*_1, \quad \text{(A.26)}$$

where $\bar{k}'_1 = \bar{k}' - G_\perp$ is the part of $\bar{k}'$ in the first Brillouin zone ($G_\perp = \sigma' G_\lambda = \tau' G_\eta$). The identity $e^{iG_\perp a} = 1$ for the reciprocal lattice vector is taken into account. The functions Λ and Φ in (A.24) and (A.25) depend on the indices σ' and τ' via their arguments.

Appendix A.2.1. Final state: below the barrier

To be more precise, only the normal to the surface component of the final neutron energy should be below the barrier. For the normal component of the final neutron wave vector inside the sample we introduce (with analogy to (A.22))

$$\bar{k}' = i\text{æ}', \qquad \text{æ}' = \sqrt{k_0^2 - k_\perp'^2}. \quad \text{(A.27)}$$

In the sums (A.24), (A.25) over σ' and τ' the main term corresponds evidently to $\sigma' = \tau' = 1$ because the others contain the factor $\gamma' = e^{-æ'a}$, which may be neglected apart from a small vicinity of the barrier, where $k'_\perp \to k_0$, $æ'a \le 1$ and γ' may approach unity. The barrier region is discussed in detail later. Note that even for $\sigma' = \tau' = 1$ only the coefficients $A'^{(L)}$ contribute to (A.24), (A.25), but not $A'^{(R)}$. Surely, it means that the neutrons coming from the left are scattered also to the left.

For the small energy transfer one may put $\mathbf{G}_\parallel = 0$ and $G_\lambda = G_\eta = 0$. Taking into account (A.20) and (A.21), we get

$$\Pi_l^{(1)} = \frac{\Lambda_l^{11}(\lambda_0, \lambda_0^*)}{2\lambda_0} = -\frac{(Q_\parallel^2 + |\lambda_0|^2)\operatorname{Im} U(\lambda_0, z)}{2|\lambda_0||z|^2},$$
$$\Pi_t^{(1)} = 0, \quad \text{(A.28)}$$

$$\Pi_{l,t}^{(2)} = \Phi_{l,t}^{11}(\lambda_0, \lambda_0^*) \frac{\operatorname{Im} U(iQ_\parallel, z)}{2Q_\parallel |z|^2} = \pm \frac{Q_\parallel \operatorname{Im} U(iQ_\parallel, z)}{2|z|^2}, \quad \text{(A.29)}$$

where

$$\lambda_0 = i(\text{æ} + \text{æ}'). \quad \text{(A.30)}$$

Note that for pure imaginary first argument $\alpha = i\gamma$ the function $\operatorname{Im} U$ is given by (A.12).

Appendix A.2.2. Final state: above the barrier

In the sums (A.24), (A.25) over σ' and τ' all terms should be considered equally important, since $\gamma' = e^{i\bar{k}'a}$ is now not a small parameter. If we neglect radiative capture, then the quantities $\bar{k}'$ and r' are real, and $|\gamma'| = 1$.

It is useful to split (A.24), (A.25) into the sums with $\sigma' = \tau'$ (where $\eta = \lambda^*$) and that with $\sigma' = -\tau'$ (where $\eta = -\lambda$)

$$\Pi_{l,t}^{(1)} = \frac{1}{|1 - r'^2\gamma'^2|^2} \left(\sum_{\sigma'} |A'_{\sigma'}|^2 \frac{\Lambda_{l,t}^{\sigma'\sigma'}(\lambda, \lambda^*)}{2i\text{æ}} + \sum_{\sigma'} A'_{\sigma'} A'^*_{-\sigma'} (\gamma')^{-\sigma'} \frac{\Lambda_{l,t}^{\sigma' -\sigma'}(\lambda, -\lambda)}{2\lambda} \right), \quad \text{(A.31)}$$

$$\Pi_{l,t}^{(2)} = \frac{\operatorname{Im} U(iq_\parallel, z)}{2q_\parallel |z|^2 |1 - r'^2\gamma'^2|^2} \left(\sum_{\sigma'} |A'_{\sigma'}|^2 \Phi_{l,t}^{\sigma'\sigma'}(\lambda, \lambda^*) + \sum_{\sigma'} A'_{\sigma'} A'^*_{-\sigma'} (\gamma')^{-\sigma'} \Phi_{l,t}^{\sigma' -\sigma'}(\lambda, -\lambda) \right). \quad \text{(A.32)}$$

For the explicit summation in (A.31) we need to know how $\Lambda_{l,t}^{\sigma'\sigma'}(\lambda, \lambda^*)$ and $\Lambda_{l,t}^{\sigma' -\sigma'}(\lambda, -\lambda)$ depend on σ'. From (A.18), with the use of symmetry properties (A.8), one can show that the quantity

$$\Lambda_{l,t}^{11}(\lambda, \lambda^*) \equiv \Lambda_{l,t}^{11}(\lambda_0, \lambda_0^*) \quad \text{(A.33)}$$

is pure imaginary, where

$$\lambda_0 = i\text{æ} + \bar{k}'_1. \quad \text{(A.34)}$$

On the other hand,

$$\Lambda_{l,t}^{-1\,-1}(\lambda, \lambda^*) \equiv \Lambda_{l,t}^{-1\,-1}(-\lambda_0^*, -\lambda_0) = \Lambda_{l,t}^{11}(\lambda_0, \lambda_0^*), \quad \text{(A.35)}$$

and

$$\Lambda_{l,t}^{1\,-1}(\lambda, -\lambda) \equiv \Lambda_{l,t}^{1\,-1}(\lambda_0, -\lambda_0),$$
$$\Lambda_{l,t}^{-1\,1}(\lambda, -\lambda) \equiv \Lambda_{l,t}^{-1\,1}(-\lambda_0^*, \lambda_0^*) = -\Lambda_{l,t}^{1\,-1\,*}(\lambda_0, -\lambda_0). \quad \text{(A.36)}$$

With the help of (A.33)-(A.36) one readily finds

$$\Pi_{l,t}^{(1)} = \frac{1}{|1 - r'^2\gamma'^2|^2} \left((1 + r'^2) \frac{\operatorname{Im} \Lambda_{l,t}^{11}(\lambda_0, \lambda_0^*)}{2\text{æ}} + 2\operatorname{Re}\left(A'_{+1} A'^*_{-1} (\gamma')^{-1} \frac{\Lambda_{l,t}^{1\,-1}(\lambda_0, -\lambda_0)}{2\lambda_0} \right) \right). \quad \text{(A.37)}$$

The sum (A.32) in a similar way results in

$$\Pi^{(2)}_{l,t} = \frac{\mathrm{Im}\, U(iq_\parallel, z)}{2q_\parallel |z|^2 |1 - r'^2\gamma'^2|^2} \Big((1 + r'^2)\Phi^{11}_{l,t}(\lambda_0, \lambda_0^*) + 2\mathrm{Re}\left(A'_{+1} A'^*_{-1} (\gamma')^{-1} \Phi^{1\,-1}_{l,t}(\lambda_0, -\lambda_0) \right) \Big), \quad \text{(A.38)}$$

where the quantity $\Phi^{11}_{l,t}(\lambda_0, \lambda_0^*)$ (A.19) is real.

The last terms in (A.37) and (A.38) have different values for backward (B) and forward (F) scattering because

$$\left[A'_{+1} A'^*_{-1} (\gamma')^{-1} \right]^B = A'^{(L)}_{+1} A'^{(L)*}_{-1} (\gamma')^{-1} = -r'(\gamma')^{-2}, \quad \text{(A.39)}$$

$$\left[A'_{+1} A'^*_{-1} (\gamma')^{-1} \right]^F = A'^{(R)}_{+1} A'^{(R)*}_{-1} (\gamma')^{-1} = -r'. \quad \text{(A.40)}$$

Appendix A.2.3. Final state: near the barrier. Resonances of penetration

With the results of the two previous subsections we are able to consider the upscattering of UCN into the regions close to the barrier, below or above.

In low vicinity of the barrier $\text{æ}' \ll \text{æ}$. Above the barrier two "vicinities" should be distinguished, "wide vicinity", where $\bar{k}' \ll k_\perp$, but $\bar{k}'a \gg 1$, and "close vicinity", where $\bar{k}'a \leq 1$.

In "wide vicinity" of the barrier, $\text{æ}'$ and $\bar{k}'$ may be treated as small parameters. Due to small energy transfer, we take $G_\lambda = G_\eta = 0$. In the approximation $\lambda \simeq \lambda_0 = i\text{æ}$ and $\eta \simeq \lambda_0^*$ eqs. (A.24) and (A.25) can be written as

$$\Pi^{(1)}_{l,t} \simeq \Xi(r', \gamma') \frac{\Lambda^{11}_{l,t}(\lambda_0, \lambda_0^*)}{2i\text{æ}}, \quad \text{(A.41)}$$

$$\Pi^{(2)}_{l,t} \simeq \Xi(r', \gamma') \Phi^{11}_{l,t}(\lambda_0, \lambda_0^*) \frac{\mathrm{Im}\, U(iQ_\parallel, z)}{2Q_\parallel |z|^2}, \quad \text{(A.42)}$$

where the factor

$$\Xi(r', \gamma') = \frac{|\gamma'|}{|1 - r'^2\gamma'^2|^2} \sum_{\sigma', \tau'} A'_{\sigma'} A'^*_{\tau'} (\gamma')^{-\sigma'/2} (\gamma'^*)^{-\tau'/2} \quad \text{(A.43)}$$

for backward and forward scattering is equal to

$$\Xi^B(r', \gamma') = \frac{|1 - r'\gamma'^2|^2}{|1 - r'^2\gamma'^2|^2}, \quad \Xi^F(r', \gamma') = \frac{|\gamma'|^2 \, |1 - r'|^2}{|1 - r'^2\gamma'^2|^2}. \quad \text{(A.44)}$$

When the final momentum $\bar{k}'$ is just above the barrier, where it is reasonable to put $r' \simeq 1$, then $\Xi^B \to 1$ and $\Xi^F \to 0$, and the corresponding barrier values of $\Pi_{l,t}$ (A.41) and (A.42) coincide with those from (A.28) and (A.29). The deviations arise only close to the points where

$$\gamma'^2 = e^{2i\bar{k}'a} = 1 \quad \Longrightarrow \quad \bar{k}'a = \pi n, \quad n = 1, 2, 3 \ldots \quad \text{(A.45)}$$

and, therefore, a difference between r' and 1 is of importance. For these energies Π^B decreases and Π^F increases up to the peak values

$$\Pi^{(1)B,F}_{l,t} \simeq \frac{1}{4} \frac{\Lambda^{11}_{l,t}(\lambda_0, \lambda_0^*)}{2i\text{æ}}, \quad \text{(A.46)}$$

$$\Pi^{(2)B,F}_{l,t} \simeq \frac{1}{4} \Phi^{11}_{l,t}(\lambda_0, \lambda_0^*) \frac{\mathrm{Im}\, U(iQ_\parallel, z)}{2Q_\parallel |z|^2}. \quad \text{(A.47)}$$

It is seen from (A.45) that these minima in Π^B and maxima in Π^F arise when the thickness of the layer is divisible by half of the neutron wavelength in the substance. Thus, the reason for the oscillation of the cross-section are the resonances of penetration through the layer.

When the final momentum is not too close to the barrier, the factors containing $\gamma' = e^{i\bar{k}'a}$ (*e.g.* $\left|1 - r'^2\gamma'^2\right|^{-2}$) strongly oscillate. With increase of the neutron final energy the amplitude of oscillations goes down because $r' \to 0$. However, in the "wide vicinity" of the barrier the oscillations are of importance. For not very thin sample these oscillations cannot be resolved and only the smoothed cross-section is of interest.

Appendix A.2.4. Smoothing over oscillations

The functions Π (A.37) and (A.38) with account of (A.39) and (A.40) oscillate due to the factors

$$\frac{1}{|1 - r'^2\gamma'^2|^2} = \sum_{l,m=0}^{\infty} r'^{2(l+m)} \, e^{2i(l-m)\bar{k}'a}, \qquad \frac{(\gamma')^{-2}}{|1 - r'^2\gamma'^2|^2} = \sum_{l,m=0}^{\infty} r'^{2(l+m)} \, e^{2i(l-m-1)\bar{k}'a}. \quad \text{(A.48)}$$

Keeping only the terms with zero indices in the exponents, we get the smoothed functions

$$\langle \Pi^{(1)B,F}_{l,t} \rangle = \frac{1}{1 - r'^4} \left((1 + r'^2) \frac{\mathrm{Im}\, \Lambda^{11}_{l,t}(\lambda_0, \lambda_0^*)}{2\text{æ}} - 2r'^n \, \mathrm{Re}\, \frac{\Lambda^{1\,-1}_{l,t}(\lambda_0, -\lambda_0)}{2\lambda_0} \right), \quad \text{(A.49)}$$

$$\langle \Pi^{(2)B,F}_{l,t} \rangle = \frac{\mathrm{Im}\, U(iq_\parallel, z)}{2q_\parallel |z|^2 (1 - r'^4)} \Big((1 + r'^2) \Phi^{11}_{l,t}(\lambda_0, \lambda_0^*) - 2r'^n \, \mathrm{Re}\, \Phi^{1\,-1}_{l,t}(\lambda_0, -\lambda_0) \Big), \quad \text{(A.50)}$$

where $n = 3$ for backward and $n = 1$ for forward scattering, and λ_0 is given by (A.34).

The smoothing is not justified in the "close vicinity" of the barrier where $\bar{k}'a \sim 1$. But since the smoothed quantities (A.49) and (A.50) have the same limiting values as (A.41) and (A.42), one may use the smoothed cross-section everywhere above the barrier.

The functions $\Lambda_{l,t}$, which enter (A.49), are disclosed from (A.18), (66) and (67) as

$$\mathrm{Im}\, \Lambda^{11}_l(\lambda_0, \lambda_0^*) = -\,\mathrm{Im} \left(\frac{(\mathbf{Q}_\parallel \mathbf{q}_\parallel + Q^{11}_\perp \lambda_0)(\mathbf{Q}_\parallel \mathbf{q}_\parallel + Q^{11\,*}_\perp \lambda_0) \, U(\lambda_0, z)}{|z|^2 (q_\parallel^2 + \lambda_0^2)} \right), \quad \text{(A.51)}$$

$$\operatorname{Im} \Lambda_t^{11}(\lambda_0, \lambda_0^*) = -\operatorname{Im}\left(\left(Q_\parallel^2 + |Q_\perp^{11}|^2 - \frac{(\mathbf{Q}_\parallel \mathbf{q}_\parallel + Q_\perp^{11}\lambda_0)(\mathbf{Q}_\parallel \mathbf{q}_\parallel + Q_\perp^{11\,*}\lambda_0)}{q_\parallel^2 + \lambda_0^2}\right)\frac{U(\lambda_0, z)}{|z|^2}\right), \tag{A.52}$$

$$\Lambda_l^{1\,-1}(\lambda_0, -\lambda_0) = -\frac{\left((\mathbf{Q}_\parallel \mathbf{q}_\parallel)^2 - (Q_\perp^{11}\lambda_0)^2\right) U(\lambda_0, z)}{|z|^2 (q_\parallel^2 + \lambda_0^2)}, \tag{A.53}$$

$$\Lambda_t^{1\,-1}(\lambda_0, -\lambda_0) = -\left(Q_\parallel^2 - (Q_\perp^{11})^2 - \frac{(\mathbf{Q}_\parallel \mathbf{q}_\parallel)^2 - (Q_\perp^{11}\lambda_0)^2}{q_\parallel^2 + \lambda_0^2}\right)\frac{U(\lambda_0, z)}{|z|^2}, \tag{A.54}$$

with

$$Q_\perp^{11} = i\text{æ} + \bar{k}', \quad \lambda_0 = i\text{æ} + \bar{k}_1'. \tag{A.55}$$

The functions $\Phi_{l,t}$, which enter (A.50), are evident from (A.19).

Appendix A.2.5. Interim conclusion

The general formula for the inelastic cross-section (62) for the initial sub-barrier neutrons is now fully defined with $\Pi_{l,t} = \Pi_{l,t}^{(1)} + \Pi_{l,t}^{(2)}$ given by (A.28) and (A.29) for the final state below the barrier ($k_\perp' < k_0$) or by (A.49) and (A.50) for that above the barrier ($k_\perp' > k_0$).

Appendix A.3. Inelastic transition probability for G = 0

In this appendix we calculate the dimensionless factor (70), which determines the inelastic transition probability (69) with momentum transfer inside the first Brillouin zone ($\mathbf{G} = 0$).

In the integral (70) it is useful to replace the variable $k_\perp'$ by $k_\parallel'^2$ and the variable φ by $Q_\parallel^2 = (\mathbf{k}_\parallel' - \mathbf{k}_\parallel)^2$ running from $(k_\parallel' - k_\parallel)^2$ up to $(k_\parallel' + k_\parallel)^2$. Thus,

$$W_{l,t}(k_\perp, k_\parallel \to \varepsilon') = \frac{k_\perp}{2\pi^2 k}\int \mathrm{d}k_\parallel'^2 \int \mathrm{d}Q_\parallel^2\, g(Q_\parallel, k_\parallel', k_\parallel)\,\frac{|t'|^2}{k_\perp'}\,\Pi_{l,t}, \tag{A.56}$$

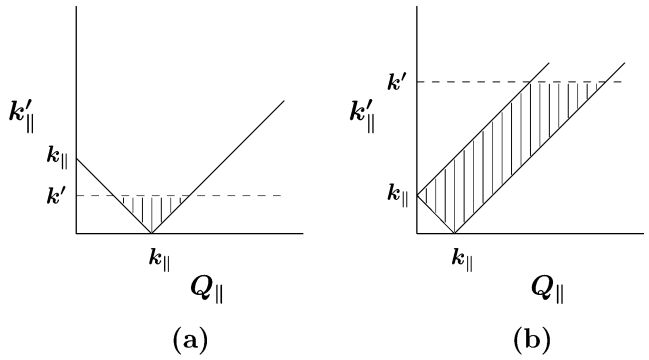

Fig. 7. Integration area for the double integral (A.56); the cases $k' < k_\parallel$ (a) and $k' > k_\parallel$ (b).

where the function g can be presented in two forms

$$g(Q_\parallel, k_\parallel', k_\parallel) = \frac{1}{\sqrt{\left((k_\parallel' + k_\parallel)^2 - Q_\parallel^2\right)\left(Q_\parallel^2 - (k_\parallel' - k_\parallel)^2\right)}} = \frac{1}{\sqrt{\left((Q_\parallel + k_\parallel)^2 - k_\parallel'^2\right)\left(k_\parallel'^2 - (Q_\parallel - k_\parallel)^2\right)}}. \tag{A.57}$$

Note that

$$|t'|^2 = \begin{cases} 4k_\perp'^2/k_0^2, & k_\perp' < k_0, \\ 4k_\perp'^2/(k_\perp' + \bar{k}')^2, & k_\perp' > k_0. \end{cases} \tag{A.58}$$

The integration area for the double integral (A.56) is shown in fig. 7.

The general formulae for the factors $\Pi_{l,t}$ are given by (A.28), (A.29) for the final state below the barrier ($k_\perp' < k_0$), and by (A.49), (A.50) for the final state above the barrier ($k_\perp' > k_0$). When $\mathbf{G} = 0$, eqs. (A.49) and (A.50) are simplified, and the sums of forward- and backward-scattering contributions can be written in the form

$$\Pi_l^{(1)} = \frac{1}{1 - r'^2}\left(-\frac{(Q_\parallel^2 + |\lambda_0|^2)\operatorname{Im} U(\lambda_0, z)}{\text{æ}|z|^2} + \frac{r'}{|z|^2}\operatorname{Re}\frac{(Q_\parallel^2 - \lambda_0^2)\,U(\lambda_0, z)}{\lambda_0}\right), \quad \Pi_t^{(1)} = 0, \tag{A.59}$$

$$\Pi_{l,t}^{(2)} = \pm\frac{Q_\parallel \operatorname{Im} U(iQ_\parallel, z)}{(1 + r')|z|^2}, \tag{A.60}$$

where $\lambda_0 = i\text{æ} + \bar{k}'$.

Appendix A.3.1. Estimations for variables and functions

The function $U(\alpha, z)$ (A.7) in (A.59) and (A.60) represents the correlation function. The real and imaginary parts of

the variable $z = x + iy$ are determined by the equations

$$2xy = \Gamma^2, \qquad y^2 - x^2 = Q_\parallel^2 - \frac{\epsilon\,\omega^2}{c^2}. \tag{A.61}$$

With the fixed initial and final neutron energies, ε and ε', the "damping factor" Γ^2 (see sect. 3) may be treated as the constant (defined by appropriate physics). The same is true for the quantity $\epsilon\,\omega^2/c^2$. It is convenient to use one of these parameters as a unit and transform all variables into the dimensionless form ($k'_\parallel \to \tilde{k}'_\parallel$, $Q_\parallel \to \tilde{Q}_\parallel$, $\Pi_{l,t} \to \tilde{\Pi}_{l,t}$ etc.). We choose as the unit $\Gamma/\sqrt{2}$, thus, *e.g.*,

$$x \to \tilde{x} = \frac{\sqrt{2}x}{\Gamma}, \quad y \to \tilde{y} = \frac{\sqrt{2}y}{\Gamma}, \quad Q_\parallel \to \tilde{Q}_\parallel = \frac{\sqrt{2}Q_\parallel}{\Gamma}, \tag{A.62}$$

and, in particular,

$$\tilde{\omega}^2 \equiv \frac{2\epsilon\,\omega^2}{\Gamma^2 c^2}. \tag{A.63}$$

Note that $\epsilon = 1$, except for the longitudinal thermo-diffusion mode (see text after (41)), where $\epsilon = 0$. In the integral (A.56) the upper limit for $\tilde{k}'^2_\parallel$ is

$$\tilde{k}'^2 = \frac{2k'^2}{\Gamma^2}. \tag{A.64}$$

Equations (A.61) take the form

$$\tilde{x}\tilde{y} = 1, \qquad \tilde{y}^2 - \tilde{x}^2 = \tilde{Q}_\parallel^2 - \tilde{\omega}^2. \tag{A.65}$$

They define the functions $\tilde{x}(\tilde{Q}_\parallel)$ and $\tilde{y}(\tilde{Q}_\parallel)$ provided the parameter $\tilde{\omega}^2$ is given. Therefore, for our problem (with fixed ε and ε'), there is only one additional parameter, $\tilde{\omega}^2$, which should be specified by the physics of the process.

The damping factors Γ^2 for longitudinal sound waves for both solids and liquids (24) and for transverse sound waves for solids (25), as a rule, are much less than k'^2. On the other hand, in the diffusion-like cases (34) and (37) the damping factor takes the form

$$\Gamma^2 = \frac{|\omega|}{D} = \frac{2m|\varepsilon' - \varepsilon|}{\hbar^2 d}, \qquad d = \frac{2mD}{\hbar}, \tag{A.66}$$

where $D = D_S$ for longitudinal thermo-diffusion for both solids and liquids, and $D = \nu$ for damping transverse waves in liquids. Parameter d is dimensionless. It means that (A.64) can be presented as

$$\tilde{k}'^2 = \frac{2\varepsilon' d}{|\varepsilon' - \varepsilon|}. \tag{A.67}$$

Note that in all realistic cases $d \gg 1$ (see sect. 7). Therefore, both for sound-like and diffusion-like modes one has

$$\tilde{k}'^2 \gg 1. \tag{A.68}$$

The following relationship

$$\tilde{\omega}^2 \ll \tilde{k}'^2, \tag{A.69}$$

is also of great importance. Indeed,

$$\frac{\omega^2}{c^2} \approx \frac{\varepsilon'^2}{\hbar^2 c^2} = \frac{\varepsilon'}{2mc^2}\,k'^2 \ll k'^2, \tag{A.70}$$

because ε' is restricted from above by the Debye energy

$$\varepsilon_D = \hbar c (6\pi^2 n)^{1/3}, \tag{A.71}$$

and $\varepsilon_D \ll 2mc^2$ for all substances.

Let us separate two regions of integration over $\tilde{Q}_\parallel$ in (A.56): (I), where $\tilde{Q}_\parallel \sim \tilde{k}' \gg 1$ and $\tilde{\omega}$ (see (A.68) and (A.69)), therefore

$$\text{(I)}: \quad \tilde{x} \ll 1 \ll \tilde{y} \sim \tilde{Q}_\parallel \sim \tilde{k}', \tag{A.72}$$

and (II), where $\tilde{Q}_\parallel \ll \tilde{k}'$, therefore (see (A.68) and (A.69))

$$\text{(II)}: \quad \tilde{x}, \tilde{y}, \tilde{Q}_\parallel \ll \tilde{k}'. \tag{A.73}$$

In region (I) the factor $\Pi^{(2)}_{l,t}$ (A.29) and (A.60) is of the scale

$$\tilde{\Pi}^{(2)}_{l,t} \sim \frac{1}{\tilde{y}^3} \sim \frac{1}{\tilde{Q}^3_\parallel} \ll 1. \tag{A.74}$$

The explicit form of the factor $\tilde{\Pi}^{(1)}_l$ in the same region depends on whether the energy transfer is small and large. For small energy transfer, $\tilde{y} \sim \tilde{Q}_\parallel \sim \tilde{k}' \sim \tilde{\varkappa}$, and one has

$$\tilde{\Pi}^{(1)}_l \sim \frac{1}{\tilde{Q}^3_\parallel} \ll 1 \tag{A.75}$$

both from (A.28) and (A.59). The case of large energy transfer corresponds to the relations: $\tilde{\varkappa} \sim \tilde{k}_0 \ll \tilde{y} \sim \tilde{Q}_\parallel \sim \tilde{k}'$. In this case only the region $k'_\perp > k_0$ is of interest. Therefore, one obtains from (A.59)

$$\tilde{\Pi}^{(1)}_l \simeq \frac{4\left(\tilde{Q}^2_\parallel + \tilde{k}'^2_\perp\right)}{\tilde{\varkappa}\left(\tilde{k}'^2_\perp + \tilde{y}^2\right)^2}. \tag{A.76}$$

Note that this term dominates due to the relatively small factor $\tilde{\varkappa}$ in its denominator.

Now let us consider region (II). The dimensionless factor $\tilde{\Pi}^{(2)}_{l,t}$ both below and above the barrier may be written in the form

$$\tilde{\Pi}^{(2)}_{l,t} = \mp\frac{\phi'\tilde{x}\tilde{Q}_\parallel(\tilde{Q}_\parallel + 2\tilde{y})}{|\tilde{z}|^2\left(\tilde{x}^2 + (\tilde{Q}_\parallel + \tilde{y})^2\right)}, \tag{A.77}$$

where

$$\phi' = \begin{cases} 1, & k'_\perp < k_0, \\ (k'_\perp + \bar{k}')/k'_\perp, & k'_\perp > k_0. \end{cases} \tag{A.78}$$

The factor (A.28), (A.59) for the small energy transfer takes the form

$$\tilde{\Pi}^{(1)}_l \simeq \frac{\phi'\tilde{x}}{|\tilde{z}|^2}. \tag{A.79}$$

But it cannot be substantially simplified for large energy transfer. However, this is of no importance. Indeed, in this case the main contribution to the cross-section comes from region (I) due to the dominating term (A.76).

Appendix A.3.2. Estimation of the integral

Let us now estimate the integral (A.56). We see that region (I) contributes only to the factor W_l for the large energy transfer due to (A.76). Since $k' \sim Q_\parallel \gg æ \sim k_\parallel$, one can perform the integration over $k'_\parallel$ in (A.56) in the narrow interval $Q_\parallel - k_\parallel < k'_\parallel < Q_\parallel + k_\parallel$ (see fig. 7b). It gives

$$W_l^{(\mathrm{I})}(k_\perp, k_\parallel \to \varepsilon') \simeq \frac{k_\perp}{2\pi k} \int \mathrm{d}\tilde{Q}_\parallel^2 \, \frac{|t'|^2}{\tilde{k}'_\perp} \, \tilde{\Pi}_l^{(1)}, \qquad (A.80)$$

where $\tilde{k}'_\perp = \sqrt{\tilde{k}'^2 - \tilde{Q}_\parallel^2}$, and $\tilde{\Pi}_l^{(1)}$ is given by (A.76). Taking into account (A.65) and (A.72) and integrating over $\tilde{Q}_\parallel^2$ from $\tilde{\omega}^2$ to $\tilde{k}'^2$, one obtains

$$W_l^{(\mathrm{I})}(k_\perp, k_\parallel \to \varepsilon') \simeq \frac{2k_\perp \Gamma^2 k'^2}{\pi k æ \left(k'^2 - \epsilon\,\omega^2/c_l^2\right)^{3/2}}, \qquad (A.81)$$

where the result is presented in terms of the physical quantities.

Now let us consider the contribution to the cross-section from region (II). It is convenient to rewrite the factor (A.56) as follows:

$$W_{l,t}(k_\perp, k_\parallel \to \varepsilon') = \frac{k_\perp}{2\pi^2 k} \int \mathrm{d}\tilde{Q}_\parallel^2 \frac{\tilde{\Pi}_{l,t}}{\phi'} \int \mathrm{d}\tilde{k}'^2_\parallel \, \tilde{g} \tilde{f}(k'_\perp), \qquad (A.82)$$

where the function $\tilde{\Pi}_{l,t}/\phi'$ given by (A.77) and (A.79) depends only on $\tilde{Q}_\parallel^2$, and

$$f(k'_\perp) \equiv \frac{\phi'|t'|^2}{k'_\perp} = \frac{4}{k_0^2} \left(k'_\perp - \theta(k'^2_\perp - k_0^2) \sqrt{k'^2_\perp - k_0^2} \right), \qquad (A.83)$$

with $\theta(x) = 0$ for $x < 0$ and $\theta(x) = 1$ for $x \geq 0$.

The integral over $\tilde{k}'^2_\parallel$ is of the form

$$\int \mathrm{d}\tilde{k}'^2_\parallel \, \tilde{g} \tilde{f}(k'_\perp) = \frac{4}{\tilde{k}_0^2} \left(I(\tilde{k}') - I(\sqrt{\tilde{k}'^2 - \tilde{k}_0^2}) \right), \qquad (A.84)$$

where

$$I(b) = \theta(b^2 - \tilde{k}_\parallel^2) \int \mathrm{d}\tilde{k}'^2_\parallel \, \tilde{g} \; \theta(b^2 - \tilde{k}'^2_\parallel) \sqrt{b^2 - \tilde{k}'^2_\parallel}. \qquad (A.85)$$

The variable $\tilde{k}'^2_\parallel$ runs from $(\tilde{Q}_\parallel - \tilde{k}_\parallel)^2$ up to $(\tilde{Q}_\parallel + \tilde{k}_\parallel)^2$ (see fig. 7). Then, $I(b)$ can be presented in terms of the elliptic integral

$$I(b) = 2\,\theta(b^2 - \tilde{k}_\parallel^2)\, \beta E\left(\frac{\alpha^2}{\beta^2}\right), \qquad E(m) = \int_0^{\pi/2} \sqrt{1 - m \sin^2\theta}\, \mathrm{d}\theta, \qquad (A.86)$$

where

$$\alpha^2 = 4\tilde{Q}_\parallel \tilde{k}_\parallel, \qquad \beta^2 = b^2 - (\tilde{Q}_\parallel - \tilde{k}_\parallel)^2. \qquad (A.87)$$

It is of importance that in region (II) for both small and large energy transfer one has

$$\tilde{Q}_\parallel \tilde{k}_\parallel \ll \tilde{k}'\tilde{k}_\parallel \leq \tilde{k}'^2 - \tilde{k}_0^2, \, \tilde{k}'^2 \quad \Longrightarrow \quad \alpha \ll \beta. \qquad (A.88)$$

Then, really $E(\alpha^2/\beta^2) \simeq \pi/2$, and, therefore, the contribution from region (II) to the cross-section is

$$W_{l,t}^{(\mathrm{II})}(k_\perp, k_\parallel \to \varepsilon') \simeq \frac{k_\perp}{2\pi k} \int \mathrm{d}\tilde{Q}_\parallel^2 \, \frac{|t'|^2}{\tilde{k}'_\perp} \, \tilde{\Pi}_{l,t}, \qquad (A.89)$$

where $\tilde{k}'_\perp = \sqrt{\tilde{k}'^2 - (\tilde{Q}_\parallel - \tilde{k}_\parallel)^2} \simeq \sqrt{\tilde{k}'^2 - \tilde{k}_\parallel^2}$, while $\tilde{\Pi}_l^{(1)}$ and $\tilde{\Pi}_{l,t}^{(2)}$ are given by (A.79) and (A.77), respectively.

To calculate the integral it is convenient to replace $\tilde{Q}_\parallel^2$ by $\tilde{x}$ with the use of

$$\mathrm{d}\tilde{Q}_\parallel^2 = -\frac{2|\tilde{z}|^2}{\tilde{x}} \, \mathrm{d}\tilde{x}. \qquad (A.90)$$

The limit $\tilde{Q}_\parallel = 0$ corresponds to

$$\tilde{x}_0^2 = \sqrt{\frac{\tilde{\omega}^4}{4} + 1} + \frac{\tilde{\omega}^2}{2}. \qquad (A.91)$$

In the opposite limit $\tilde{Q}_\parallel \to \infty$, $\tilde{x} \to 0$, then the integral (A.89) can be presented in the form

$$W_l^{(\mathrm{II})}(k_\perp, k_\parallel \to \varepsilon') = \frac{k_\perp}{\pi k} \, \tilde{f}(k'_\perp) \left(\tilde{J}^{(1)} - \tilde{J}^{(2)} \right), \qquad (A.92)$$

$$W_t^{(\mathrm{II})}(k_\perp, k_\parallel \to \varepsilon') = \frac{k_\perp}{\pi k} \, \tilde{f}(k'_\perp) \, \tilde{J}^{(2)}, \qquad (A.93)$$

where

$$\tilde{J}^{(1)} = \tilde{x}_0, \quad \tilde{J}^{(2)} = \int_0^{\tilde{x}_0} \frac{\tilde{Q}_\parallel(\tilde{Q}_\parallel + 2\tilde{y})}{\tilde{x}^2 + (\tilde{Q}_\parallel + \tilde{y})^2} \, \mathrm{d}\tilde{x}. \qquad (A.94)$$

Straightforward calculation gives

$$\tilde{J}^{(2)} = \frac{2\tilde{x}_0}{3}. \qquad (A.95)$$

Then, summing the contributions from regions (I) and (II) we get in terms of the physical quantities the results (74)-(78).

Appendix A.4. Inelastic transition probability for $\mathbf{G} \neq \mathbf{0}$

In this appendix we calculate the dimensionless factor (73) which determines the inelastic transition probability (72) with the momentum transfer $\mathbf{G}$ to the crystal lattice. The final neutron energy $\varepsilon' \simeq \hbar^2 G^2/2m$ is much larger than the barrier energy U and initial energy ε, thus

$$\mathbf{k}'_\parallel \simeq -\mathbf{G}_\parallel, \quad \bar{k}' \simeq k'_\perp \simeq G_\perp \gg æ, \quad r' \to 0, \quad t' \to 1. \qquad (A.96)$$

The Π factors (A.49) and (A.50) have now equal contributions from backward and forward scattering and, with the help of approximations (A.96) and expression (A.51)-(A.55), (A.19), take the form

$$\Pi_l^{(1)} = -\frac{1}{æ|z|^2}\,\mathrm{Im}\left(\frac{\left(\mathbf{G}_\parallel\mathbf{q}_\parallel + G_\perp\lambda_0\right)^2 U(\lambda_0,z)}{q_\parallel^2+\lambda_0^2}\right), \tag{A.97}$$

$$\Pi_t^{(1)} = -\frac{G^2\,\mathrm{Im}\,U(\lambda_0,z)}{æ|z|^2} + \frac{1}{æ|z|^2}\,\mathrm{Im}\left(\frac{\left(\mathbf{G}_\parallel\mathbf{q}_\parallel+G_\perp\lambda_0\right)^2 U(\lambda_0,z)}{q_\parallel^2+\lambda_0^2}\right), \tag{A.98}$$

$$\Pi_{l,t}^{(2)} = \pm\frac{q_\parallel^2|\mathbf{G}_\parallel\mathbf{q}_\parallel + G_\perp\lambda_0|^2 - |\lambda_0\mathbf{G}_\parallel\mathbf{q}_\parallel - G_\perp q_\parallel^2|^2}{|q_\parallel^2+\lambda_0^2|^2} \times\frac{\mathrm{Im}\,U(iq_\parallel,z)}{q_\parallel|z|^2}, \tag{A.99}$$

where

$$\lambda_0 = iæ + \xi_\perp, \qquad \xi_\perp = k'_\perp - G_\perp. \tag{A.100}$$

The integral (73) is over the Brillouin zone with the center in $\mathbf{G}$. It is convenient to take

$$\mathrm{d}^3k' = \mathrm{d}k'_\perp\mathrm{d}^2k'_\parallel \to \mathrm{d}\xi_\perp\mathrm{d}^2q_\parallel, \tag{A.101}$$

because $\mathbf{q}_\parallel = -\mathbf{k}'_\parallel - \mathbf{G}_\parallel$. Integration over the angle between $\mathbf{q}_\parallel$ and $\mathbf{G}_\parallel$ gives

$$\langle\mathbf{G}_\parallel\mathbf{q}_\parallel\rangle = 0, \qquad \langle\left(\mathbf{G}_\parallel\mathbf{q}_\parallel\right)^2\rangle = \frac{G_\parallel^2q_\parallel^2}{2}. \tag{A.102}$$

Then the W factors take the form

$$W_{l,t}^{(1)}(k_\perp, k_\parallel\to\mathbf{G}) = \frac{k_\perp}{\pi kæG^2}\int\mathrm{d}\xi_\perp\mathrm{d}q_\parallel^2 \times\left(\mp\frac{q_\parallel^2\left(G_\parallel^2/2-G_\perp^2\right)}{|z|^2}\,\mathrm{Im}\left(\frac{U(\lambda_0,z)}{q_\parallel^2+\lambda_0^2}\right) - \frac{G_{\perp,\parallel}^2\,\mathrm{Im}\,U(\lambda_0,z)}{|z|^2}\right), \tag{A.103}$$

$$W_{l,t}^{(2)}(k_\perp, k_\parallel\to\mathbf{G}) = \pm\frac{k_\perp}{\pi kG^2}\int\mathrm{d}\xi_\perp\mathrm{d}q_\parallel^2 \times\frac{q_\parallel\left(G_\parallel^2/2-G_\perp^2\right)(q_\parallel^2-|\lambda_0|^2)\,\mathrm{Im}\,U(iq_\parallel,z)}{|z|^2|q_\parallel^2+\lambda_0^2|^2}. \tag{A.104}$$

Now we can integrate over $\xi_\perp$ transforming the integrals into contour ones by closing a path in the complex $\xi_\perp$-plane. For three functions to be integrated, one easily obtains

$$\int\mathrm{d}\xi_\perp\,\mathrm{Im}\left(\frac{U(\lambda_0,z)}{q_\parallel^2+\lambda_0^2}\right) = \begin{cases}0, & q_\parallel<æ,\\ \pi\,\mathrm{Im}\,U(iq_\parallel,z)/q_\parallel, & q_\parallel>æ,\end{cases} \tag{A.105}$$

$$\int\mathrm{d}\xi_\perp\,\mathrm{Im}\,U(\lambda_0,z) = -2\pi x, \tag{A.106}$$

$$\int\mathrm{d}\xi_\perp\frac{q_\parallel^2-|\lambda_0|^2}{|q_\parallel^2+\lambda_0^2|^2} = \begin{cases}-\pi/æ, & q_\parallel<æ,\\ 0, & q_\parallel>æ.\end{cases} \tag{A.107}$$

Using these results we get for the sum of $W^{(1)}$ and $W^{(2)}$ factors

$$W_{l,t}(k_\perp, k_\parallel\to\mathbf{G}) = \mp\frac{k_\perp\left(G_\parallel^2/2-G_\perp^2\right)}{kæG^2} \times\int\mathrm{d}q_\parallel^2\frac{q_\parallel\,\mathrm{Im}\,U(iq_\parallel,z)}{|z|^2} + \frac{2k_\perp G_{\perp,\parallel}^2}{kæG^2}\int\mathrm{d}q_\parallel^2\frac{x}{|z|^2}. \tag{A.108}$$

Using (A.12) and (A.90), one obtains

$$\int\mathrm{d}q_\parallel^2\frac{q_\parallel\,\mathrm{Im}\,U(iq_\parallel,z)}{|z|^2} = -4J^{(2)}, \tag{A.109}$$

$$\int\mathrm{d}q_\parallel^2\frac{x}{|z|^2} = 2J^{(1)}, \tag{A.110}$$

where $J^{(1)}$ and $J^{(2)}$ are given by (A.94) and (A.95). Thus, the W factors are of the form (79) and (80).

References

1. V.I. Luschikov, Y.N. Pokotilovsky, A.V. Strelkov, F.L. Shapiro, JETP Lett. **9**, 23 (1969).
2. A. Steyerl, Phys. Lett. B **29**, 33 (1969).
3. R. Golub, Rev. Mod. Phys. **68** 329 (1996).
4. E. Korobkina, R. Golub, J. Butterworth, P. Geltenbort, S. Arzumanov, Phys. Rev. B **70** 035409 (2004).
5. A.V. Strelkov, V.V. Nesvizhevsky, P. Geltenbort, D.G. Kartashov, A.G. Kharitonov, E.V. Lychagin, A.Yu. Muzychka, J.M. Pendlebury, K. Schreckenbach, V.N. Shvetsov, A.P. Serebrov, R.R. Taldaev, P. Yaidjiev, Nucl. Instrum. Methods A **440**, 695 (2000).
6. L.N. Bondarenko, P. Geltenbort, E.I. Korobkina, V.I. Morozov, Yu.N. Panin, Phys. At. Nucl. **65**, 11 (2002).
7. E.V. Lychagin, D.G. Kartashov, A.Yu. Muzychka, V.V. Nesvizhevsky, G.V. Nekhaev, A.V. Strelkov, Phys. At. Nucl. **65**, 1995 (2002).
8. A. Steyerl, B.G. Yerozolimsky, A.P. Serebrov, P. Geltenbort, N. Achiwa, Yu.N. Pokotilovski, O. Kwon, M.S. Lasakov, I.A. Krasnoshchokova, A.V. Vasilyev, Eur. Phys. J. B **28**, 299 (2002).

9. A.P. Serebrov, J. Butterworth, M. Daum, A.K. Fomin, P. Geltenbort, K. Kirch, I.A. Krasnoschekova, M.S. Lasakov, Yu.P. Rudnev, V.E. Varlamov, A.V. Vassiljev, Phys. Lett. A **309**, 218 (2003).
10. L. Van Hove, Phys. Rev. **95**, 249 (1954).
11. I.I. Gurevich, L.V. Tarasov, *Low-Energy Neutron Physics* (North Holland Publ. Co., Amsterdam, 1968).
12. S.W. Lovesey, *Theory of Neutron Scattering from Condensed Matter*, Vols. **1** and **2** (Clarendon Press, Oxford, 1984).
13. A.L. Barabanov, S.T. Belyaev, Eur. Phys. J. B **15**, 59 (2000).
14. V.K. Ignatovich, *The Physics of Ultracold Neutrons* (Clarendon Press, Oxford, 1990).
15. R. Golub, D. Richardson, S.K. Lamoreaux, *Ultra-cold Neutrons* (Adam Hilger, Bristol, 1991).
16. D.I. Blokhintzev, N.M. Plakida, Phys. Status Solidi B **82**, 627 (1977); preprint JINR P4-9631 (JINR, Dubna, 1976) (in Russian); preprint JINR P4-10381 (JINR, Dubna, 1977) (in Russian).
17. V.K. Ignatovich, M. Utsuro, Nucl. Instrum. Methods A **440**, 709 (2000).
18. A. Serebrov, N. Romanenko, O. Zherebtsov, M. Lasakov, A. Vasiliev, A. Fomin, P. Geltenbort, I. Krasnoshekova, A. Kharitonov, V. Varlamov, Phys. Lett. A **335**, 327 (2005).
19. A.L. Barabanov, K.V. Protasov, Phys. Lett. A **346**, 378 (2005).
20. M. Daum, P. Geltenbort, R. Henneck, K. Kirch, nucl-ex/0510041.
21. Yu.N. Pokotilovski, Eur. Phys. J. B **8**, 1 (1999).
22. Yu.N. Pokotilovski, Phys. Lett. A **255**, 173 (1999).
23. S.K. Lamoreaux, R. Golub, Phys. Rev. C **66**, 044309 (2002).
24. P. Schofield, in *Physics of Simple Liquids*, edited by H.N.V. Temperley, J.S. Rowlinson, G.S. Rushbrooke (North-Holland Publishing Company, Amsterdam, 1968).
25. D. Forster, *Hydrodynamic Fluctuations, Broken Symmetry, and Correlation Functions* (W.A. Benjamin, Inc., Advanced Book Program Reading, Mass., London, Amsterdam, Don Mills, Ontario, Sidney, Tokyo, 1975).
26. A.I. Akhiezer, S.V. Peletminskii, *Methods of Statistical Physics* (Pergamon Press, Oxford, New York, 1981).
27. L.D. Landau, E.M. Lifshitz, A.P. Pitaevskii, *Statistical Physics*, Vol. **2** (Pergamon Press, Oxford, New York, 1986).
28. L.D. Landau, E.M. Lifshitz, A.M. Kosevich, L.P. Pitaevskii, *Theory of Elasticity* (Pergamon Press, Oxford, New York, 1986).
29. B.Ya. Balagurov, V.G. Vaks, Zh. Eksp. Teor. Fiz. **57**, 1646 (1969).
30. Ia.I. Frenkel', *Kinetic Theory of Liquids* (Clarendon Press, Oxford, 1946).
31. V.V. Nesvizhevsky, Phys. At. Nucl. **65**, 400 (2002).